CHAPTER 5

# CHARACTERIZATION OF ASPHALT BINDERS

## 5.1 Preface

Considering their capability in minimizing the Greenhouse gas emissions (GHG) and resulting global warming issues, warm mix asphalt (WMA) is gaining popularity all over the globe owing to the low mixing and compaction temperatures. Reduction in production temperatures also leads to lower ageing temperature and reduced oxidative hardening of asphalt binder [242,280]. However, in contrast to such benefits, maintaining the similar performance of WMA binders, as conventional binders, is a critical research challenge. The potential concerns associated with WMA include their performance against rutting, fatigue, and moisture damage. Rutting is predominant during the initial phase of the pavement, while after several years of traffic loading, fatigue cracking becomes more dominant. These failures are further exacerbated due to the action of moisture. Moisture action is an external variable that intends to influence the interaction between the asphalt binder and aggregate matrix at any given loading condition. Needless to say, all these failures initiate and propagate through the binder phase of the asphalt composite. Therefore, asphalt binder, an essential and weakest zone of asphalt mixture, significantly influence pavement performance depending on temperature. The temperature dependency of asphalt binders can be explained in terms of failure types [534–536]: (a) rutting failure is more likely to occur at high temperatures due to the softening of asphalt binder, (b) fatigue cracking usually arises at intermediate temperatures due to the stiffening of asphalt binder, and (c) moisture damage manifests due to the attack of moisture on asphalt binder-aggregate interface at

average service temperature. An ideal asphalt binder is one that can resist all these critical failures over the in-service life.

This chapter demonstrates the effect of WMA technologies on the performance of base asphalt binders (VG30 and PMB40). The ageing behavior of WMA binders at reduced ageing temperature has also been discussed and compared with respective base asphalt binders. A series of tests including frequency sweep (FS), multiple stress creep and recover (MSCR), and Linear amplitude sweep test (LAST), were performed to assess the rutting and fatigue characteristics of asphalt binders. The response of the MSCR test (non-recoverable creep compliance, $J_{nr}$) was further modeled using the Arrhenius equation. This approach was used to rank different asphalt binders, irrespective of stress levels and test temperatures. Moisture resistance was evaluated based on the bond strength mechanism using Pneumatic adhesion test (PAT). A wide range of test temperatures (10-70°C) was chosen to assess the behavior of WMA in a more holistic way. Different test conditions such as frequency, ageing condition, stress/strain levels, and temperatures were chosen based on the test method, to critically understand the influence of WMA technologies on the performance of asphalt binder. The general procedure and testing approach of different test methods for assessing the ageing, rutting, fatigue, and moisture characteristics of asphalt binders have been specified in Chapter 3. This chapter intends to provide the knowledge on the relative performance of WMA binders with respect to different failure modes.

In the present study, the samples were categorized into four different groups based on the type of base asphalt binder and aggregate source. These groups are (1) Granite and VG30 (GVG), (2) Granite and PMB40 (GP), (3) Dolomite and VG30 (DVG), and (4) Dolomite and PMB40 (DP). Further, selected WMA additives (at their optimum

dosage) were added to these groups and different notations were specified for each combination, as shown in Figure 5.1. For example, addition of Aspha-Min with VG30 and granite aggregate was denoted as GAm whereas Aspha-Min with VG30 and dolomite aggregate was named as DAm. Similar nomenclatures were defined for other combinations of asphalt mixtures and the same has been followed during the study. It should be noted that the analysis of ageing, rutting, and fatigue at the binder level corresponding to GP (Granite + PMB40 + WMA) and DP (Dolomite + PMB40 + WMA) was kept the same (with notation GP/DP) throughout the chapter. This is because the optimum dosage of WMA additives with PMB40 was similar for both the aggregates (granite and dolomite) (as shown in Table 4.8).

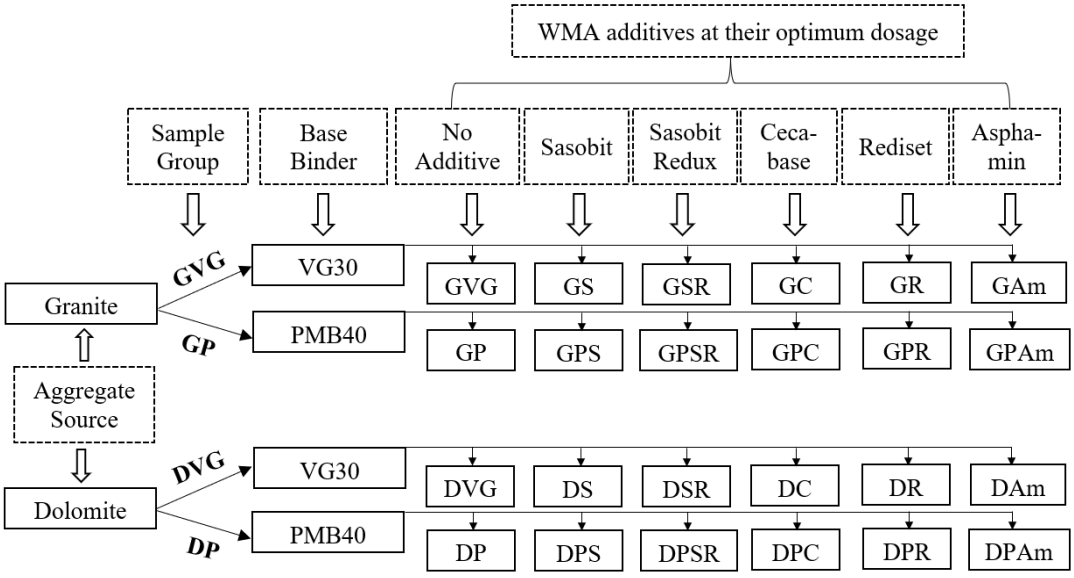


Figure 5.1. Nomenclature of sample with different base asphalt binder, aggregate source, and WMA technology

## 5.2 Ageing Behavior of WMA Binders

From the production to the in-service life of asphalt pavements, asphalt binder (or asphalt mixture) is subjected to a series of complex physiochemical progressions,

including oxidation, polymerization, syneresis, volatilization, evaporation, dehydrogenation, condensation, steric hardening, and many more, leading to the stiffening of asphalt binder. This stiffening effect or the hardening phenomenon is termed ageing. This influences the physical and chemical properties of the asphalt binder along with the mechanical behavior of asphalt mixtures[218,254,468,537].

Ageing of asphalt binder or mixtures occurs in two stages, i.e., short-term ageing (during the production process) (STA) and long-term ageing (during the in-service life under different atmospheric conditions) (LTA) [538]. Ageing itself is not any failure/distress; rather, it mobilizes or facilitates the early onset and propagation of distresses (rutting and fatigue). In addition, excessive hardening may affect the interfacial adhesion between the asphalt binder and aggregate, increasing the moisture damage propensity. Tauste et al [469] reviewed previous literatures on ageing mechanisms and highlighted that the influence of STA and LTA depends on the binder chemistry, binder grade, film thickness, aggregate gradation, aggregate source, bitumen content, production temperature, and a few others. This dependency and respective quantification of ageing become more complex when the asphalt binder is aged at reduced temperatures, as in the case of WMA [539]. It is hypothesized that WMA binders and mixtures exhibit lower stiffness or increased susceptibility to permanent deformation due to reduced ageing. Also, lower production temperatures of WMA increased the concerns about fatigue and moisture failure. At present, very few studies have evaluated the effect of reduced temperatures on the ageing behavior of WMA, considering VG30 and PMB40 as the base asphalt binder. This forms the motivation to conduct an extensive study in this direction.

Ageing process strongly influences the chemical composition of the asphalt binder. The functional group present in the asphalt binder interacts with free oxygen and transforms the generic fractions such as maltenes to high molecular weight molecules i.e., asphaltenes [469,540]. This transformation leads to increased stiffness of the asphalt binder and imparts brittle characteristics to the asphalt mix. Various compounds such as sulfoxides, anhydrides, carboxylic acid, and ketones were formed during the ageing process [469,540]. Among them, carbonyl (a group of carboxylic acid and ketone) and sulfoxides were known to be the prominent functional groups that reflect the ageing of asphalt binder. The change in these groups is usually quantified based on the intensity of their intrinsic peaks (carbonyl or sulfoxide). The quantitative analysis of the peaks corresponding to the carbonyl group (1700 $cm^{-1}$) and sulfoxide group (1030 $cm^{-1}$) can be effectively determined by studying the Fourier transform infrared (FTIR) spectrum [76,541]. FTIR is one of the simple, fastest, and most reliable techniques used by various researchers [76,214] to assess the change in the ageing behavior of unmodified as well as modified asphalt binders at the molecular level. The working mechanism of FTIR is demonstrated in Chapter 3.

Previous literature [76,218,468,541] suggested calculating different indices based on the area around the peaks of interest (1700 $cm^{-1}$ and 1030 $cm^{-1}$), as shown in Equation 5.1 and 5.2. These indices are popularly known as carbonyl index ($I_{C=O}$) and sulfoxide index ($I_{S=O}$), whose higher value indicates higher ageing susceptibility.

$$I_{C=O} = \frac{A_{1660-1800}}{A_{1350-1525}} \tag{5.1}$$

$$I_{S=O} = \frac{A_{1010-1070}}{A_{1350-1525}} \tag{5.2}$$

Where $A_{1660\text{-}1800}$ is the area around the carbonyl peak (1700 $cm^{-1}$), $A_{1010\text{-}1090}$ denotes the area around the sulfoxide peak (1030 $cm^{-1}$), and $A_{1350\text{-}1525}$ is taken as the reference area under the spectral band ranging from 1350-1525 $cm^{-1}$. This area (reference) is insensitive to the effect of ageing and is recommended in past literatures for quantifying ageing characteristics [214].

Figures 5.2 (a-c) and Figure 5.2 (d-f) present the value of $I_{C=O}$ and $I_{S=O}$, respectively, for different combinations of base asphalt binder and WMA technology at STA and LTA conditions. On an average, $I_{S=O}$ yields relatively higher values than $I_{C=O}$. This is because, during the oxidation process, the free oxygen reacts with perhydroaromatics and transforms into hydroperoxides, leading to faster and higher sulfoxides compared to the carbonyl group [76,469]. In general, a higher value of $I_{C=O}$ and $I_{S=O}$ reflects a higher ageing effect and is not desirable for durable asphalt pavement [541]. This attribution was confirmed by $I_{C=O}$ (Figure 5.2 (a-c)), indicating an upward shift with the change in ageing conditions from STA to LTA. However, $I_{S=O}$ failed to differentiate the ageing effect for a few WMA binders, as shown in Figure 5.2 (d-f). For example, the $I_{S=O}$ value for Sasobit Redux in VG30 was calculated to be 0.19 at STA condition; on the other hand, the value of $I_{S=O}$ drop-down to 0.15 at LTA condition, which is unexpected or inappropriate. Such discrepancies were observed for different combinations of WMA, such as Sasobit with VG30 and Sasobit Redux with both VG30 and PMB40. These observations are in agreement with a couple of the previous studies [542,543], which reported inconsistent trends for $I_{S=O}$ and stated that sulfoxide index might not ideally represent the ageing behavior, especially for modified asphalt binder. For this reason, $I_{S=O}$ has not been considered in the present study for further interpretation of ageing behavior.

Based on $I_{C=O}$ values, PMB40 indicated higher ageing resistance compared to VG30. In PMB, polymer fractions have a tendency to swell at high heating temperatures, which restricts the interaction between free oxygen and asphalt binder molecules. This hindrance reduced the oxidation effect and thus delayed the ageing process compared to unmodified asphalt binders (VG30 here) [204]. However, adding WMA additives (irrespective of their type) may influence the apparent trends observed for base asphalt binders. The relative change in $I_{C=O}$ highlighted the strong influence of WMA technology on the ageing behavior of base asphalt binders. All the WMA binders tend to slow down the chemical reaction and thus resulted in a similar or weak oxidation phenomenon. This is attributed to the lower ageing temperature of WMA binders in comparison to their respective base asphalt binders. However, the extent of variation in ageing effect during STA and LTA was found to be binder specific. It was observed that the influence of WMA additives depends on the ageing condition as well. WMA additives with VG30 lowered the ageing effect by around 24-65% (41-59% for STA and 24-65% for LTA), whereas 23-57% reduction (23-38% for STA and 37-57% for LTA) was observed in the case of PMB40.

As per the previous literatures [544–546], the value of $I_{C=O}$ appreciably correlates with the ageing behavior of the asphalt mixtures. Thus, it was presumed that the ageing resistance offered by the WMA additives at binder level may be equivalent to the ageing behavior at the mixture level [545,547]. Table 5.1 shows the percent reduction (relative to respective base asphalt binder) in $I_{C=O}$ for all the WMA sample groups/combinations considered in the present study (outlined in Figure 5.1). As can be seen, all the WMA combinations displayed a low value of $I_{C=O}$ and are expected to be less prone to the ageing effect. These interpretations were consistent for both the ageing conditions. Besides, the interaction between the WMA additives and base asphalt binder was vital

in influencing the ageing behavior. The use of organic additives with granite and VG30 reduced the ageing susceptibility by 24-38% for LTA conditions, while the application of chemical additives indicated 61-64% lower LTA effect on the asphalt mixtures. Similar observations were noted for other combinations and are displayed in Table 5.1. These interpretations were based on the optimum dosage of WMA additives categorized depending on the aggregate source and base asphalt binder (as shown in Chapter 4). It should be noted that no definite trend was observed with the change in WMA technology; nonetheless, all the WMA binders act as an anti-oxidant for base asphalt binders. On the other hand, it is hypothesized that the reduced ageing of WMA binders may affect their performance at binders as well as mixtures level and thus necessitates further investigations.

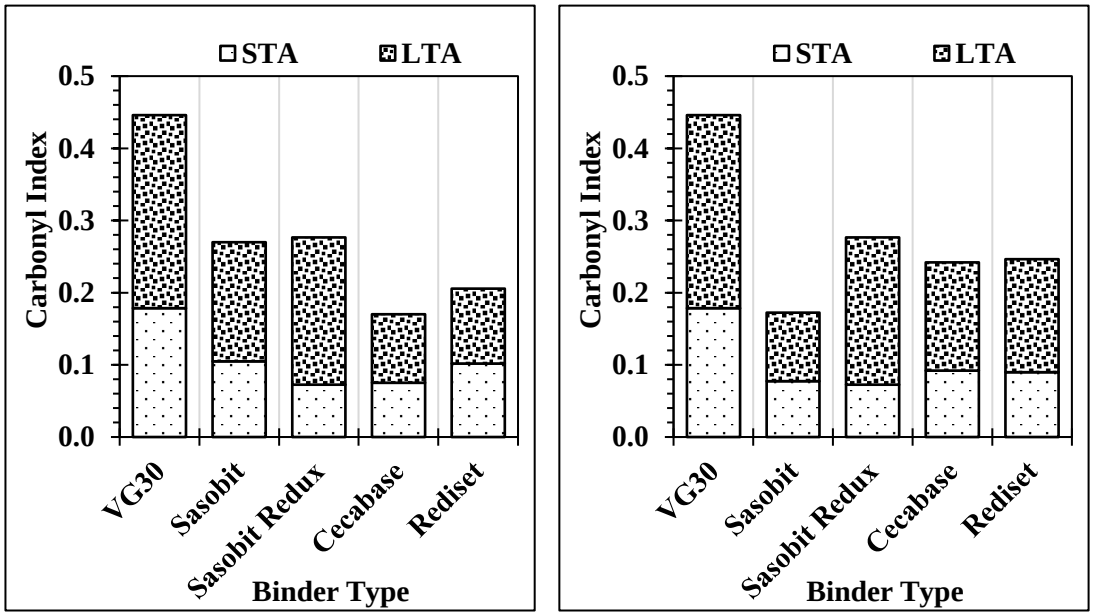


(a) (b)

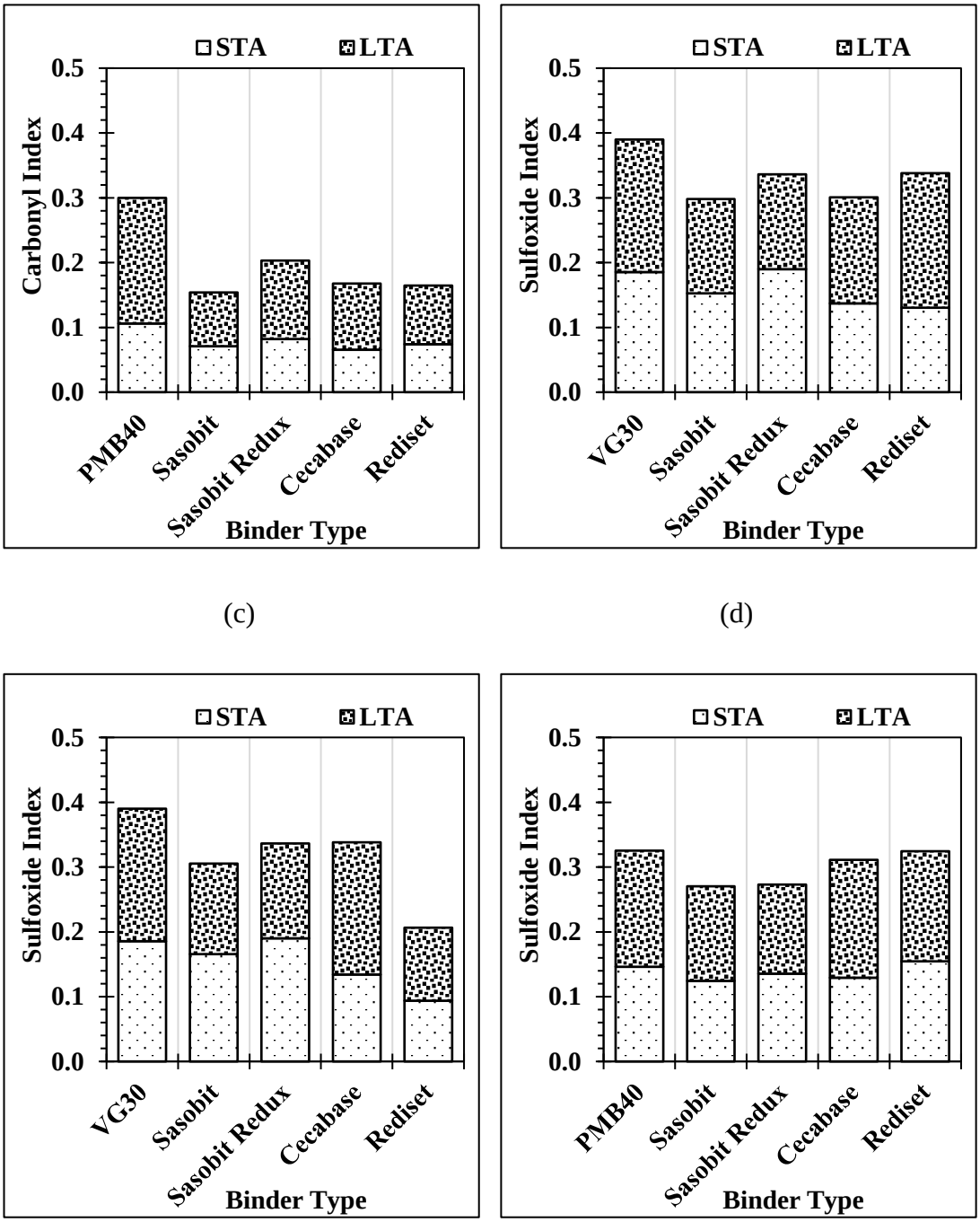


Figure 5.2. Ageing indices for different groups (a) $I_{C=O}$ for GVG, (b) $I_{C=O}$ for DVG, (c) $I_{C=O}$ for GP/DP, (d) $I_{S=O}$ for GVG, (d) $I_{S=O}$ for DVG, and (f) $I_{S=O}$ for GP/DP

Table 5.1. Expected percent improvement in ageing resistance for different combinations of asphalt mixtures

| WMA Sample Group | WMA Technology | | | |
|---|---|---|---|---|
| | Organic | | Chemical | |
| | STA | LTA | STA | LTA |
| **GVG** (Granite + VG30 + WMA) | 41-59% | 24-38% | 43-58% | 61-64% |
| **DVG** (Dolomite + VG30 + WMA) | 57-59% | 24-65% | 48-50% | 41-44% |
| **GP/DP** (Granite/Dolomite + PMB40 + WMA) | 23-33% | 37-57% | 30-38% | 47-53% |

## 5.3 Discussion on the Master Curve

Rutting and fatigue cracking are among the major distresses that lead to the premature failure of the asphalt pavements [468,548]. Rutting (permanent deformation) often occurs at high temperatures due to the softening of asphalt binder [501], whereas fatigue cracking arises due to the embrittlement of the asphalt binder at intermediate temperatures [549]. This shows that the dependency of asphalt binder on the temperature substantially influences the stiffness of asphalt pavements and so the mechanical performance. The rheological behavior of asphalt binder, which acts as an indicator of mechanical performance, can be predicted through dynamic mechanical analysis, using a dynamic shear rheometer (DSR) [550,551].

Over the years, Superpave parameters ($|G^*|/\sin\delta$ and $|G^*|\sin\delta$) has been used to characterize the rutting and fatigue potential, respectively. $G^*$ and δ signify the complex modulus value and phase lag of the asphalt binder, respectively. Frequency sweep (FS) is one of the commonly used test method to describe the rheological behavior of asphalt binders based on $|G^*|/\sin\delta$ and $|G^*|\sin\delta$. These parameters are derived based on the

concept of dissipated energy when the binder is subjected to oscillatory loading in a DSR.

The frequency sweep test was conducted using the following test protocol:

*Test Temperature:* 10, 20, 30, 40, 50, 60 and 70 °C.

*Spindle specification:* 8 mm diameter and 2 mm gap for 10-30 °C.

25 mm diameter and 1 mm gap for 40-70 °C.

*Strain:* Kept under the linear viscoelastic (LVE) limit at each temperature.

*Master Curve:* Superpave rutting parameter ($|G^*|/\sin\delta$) and fatigue parameter ($|G^*|\sin\delta$).

Master curves were plotted by shifting the data obtained at various temperatures to a single reference temperature, using time temperature superposition principle. In the present study, master curves were constructed at 20 °C and 60 °C to estimate the fatigue and rutting potential of the asphalt binders respectively. With reference to the PG system, $|G^*|/\sin\delta$ master curve was analysed for STA asphalt binders at 60 °C, while $|G^*|\sin\delta$ master curve was analysed for LTA asphalt binders at 20 °C. A higher value of $|G^*|/\sin\delta$ and a lower value of $|G^*|\sin\delta$ is desirable for better rutting and fatigue resistance, respectively.

Figure 5.3 and 5.4 present the $|G^*|/\sin\delta$ and $|G^*|\sin\delta$ master curves constructed for different sample groups at reference temperatures of 60 °C and 20 °C, respectively. As can be seen, addition of WMA additives does not influence the rutting characteristics of base asphalt binders, except Sasobit. Attributed to the crystallization of wax, Sasobit binders showed higher value of $|G^*|/\sin\delta$, leading to improved rutting susceptibility [207]. However, its effect was observed to be more prominent at lower frequency range. With the increase in frequency, master curve of Sasobit tends to coincide with the base asphalt binder and thus indicated comparable performance at higher frequency range.

Interestingly, the influence of Sasobit was found to be insignificant in case of PMB40. Since $|G^*|/\sin\delta$ master curves were plotted for STA binders, it can be stated that WMA binders perform satisfactorily (similar or even better than base binders) in terms of rutting resistance even at lower ageing temperatures.

From Figure 5.4, it can be perceived that WMA binders showed either similar or higher $|G^*|\sin\delta$ than base asphalt binders. In general, higher value of $|G^*|\sin\delta$ is not desirable from the fatigue point of view. It was found that few WMA binders in VG30, particularly organic-based, lead to higher fatigue susceptibility owing to their crystallization effect [246]. On the other hand, the difference in fatigue parameter $|G^*|\sin\delta$ was not found to be negligible in case of PMB40. Similar to $|G^*|/\sin\delta$, the variation in the master curves was more pronounced at lower frequency range. Notably, fatigue is more critical for fast moving vehicles, which is explained by higher frequency range. Based on the master curves, all the WMA binders displayed similar results as base asphalt binders at relatively higher frequencies.

Statistical analysis using analysis of variance was performed to check the statistical difference between WMA binders and base asphalt binders based on $|G^*|/\sin\delta$ and $|G^*|\sin\delta$ values at a frequency of 10 rad/sec. The p-value was determined considering a confidence level of 95%. As per the analysis, some of the WMA binders showed higher values than 0.05, while some of them indicated lower values. On an average, the results obtained from analysis of variance indicated that the effect of WMA additives in VG30 was significant ($p>0.05$), whereas their influence in PMB40 was found to be insignificant ($p<0.05$). This shows that the impact of WMA binders is highly dependent on the type of WMA technology and base asphalt binder. In addition, the analysis of rutting and fatigue parameter master curve confirmed that the influence of WMA binders is also a function of loading rate or frequency. It should be noted that the results

of $|G^*|/\sin\delta$ and $|G^*|\sin\delta$ may not be very effective/reliable as these parameters are merely dependent on the stiffness of the asphalt binder. For example, adding Sasobit in VG30 enhance the stiffness, which is desirable for rutting but inadequate for fatigue. This showed that stiffness alone may not truly describe the complicated viscoelastic behaviour of asphalt binders. In addition, FS test was conducted under the linear viscoelastic region; nonetheless, the influence of WMA might change under non-linear viscoelastic regions. Thus, advanced tests such as MSCR and LAST are recommended to clearly comprehend the rutting and fatigue behavior of WMA binders under linear and non-linear regimes.

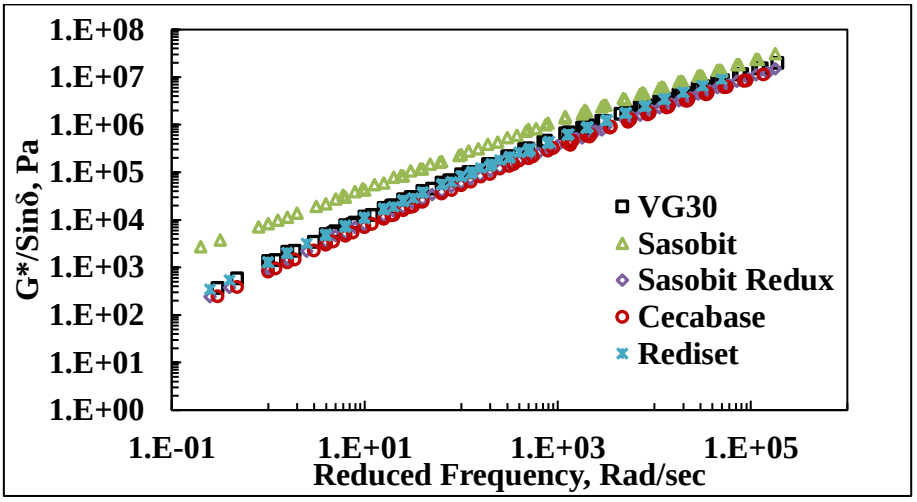


(a)

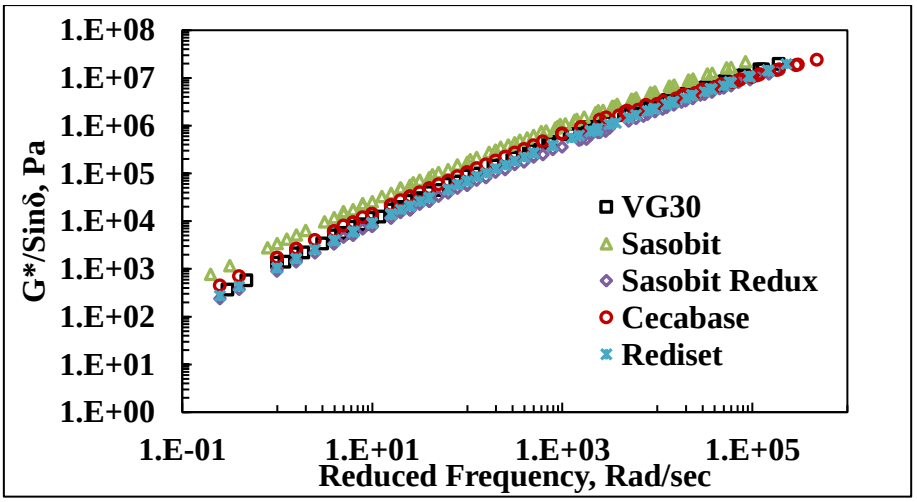


(b)

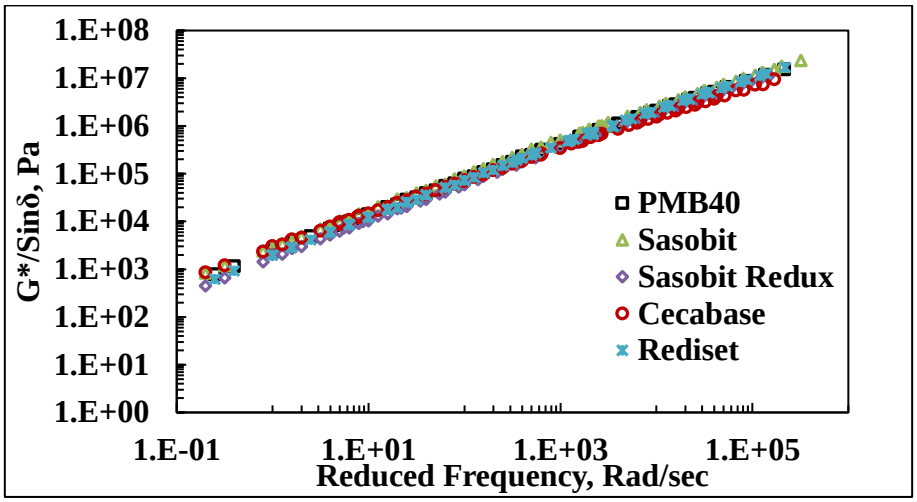


(c)

Figure 5.3. $|G^*|/\sin\delta$ master curves at 60°C for different sample groups (a) GVG, (b) DVG, and (c) GP/DP

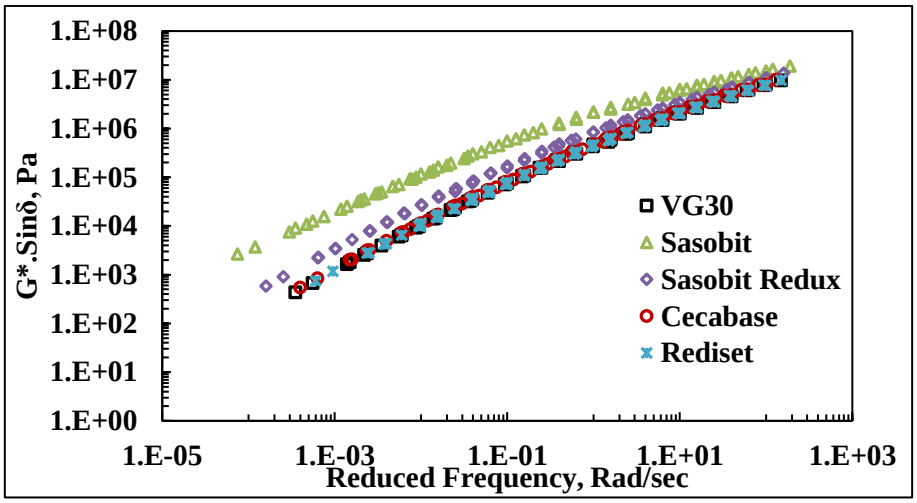


(a)

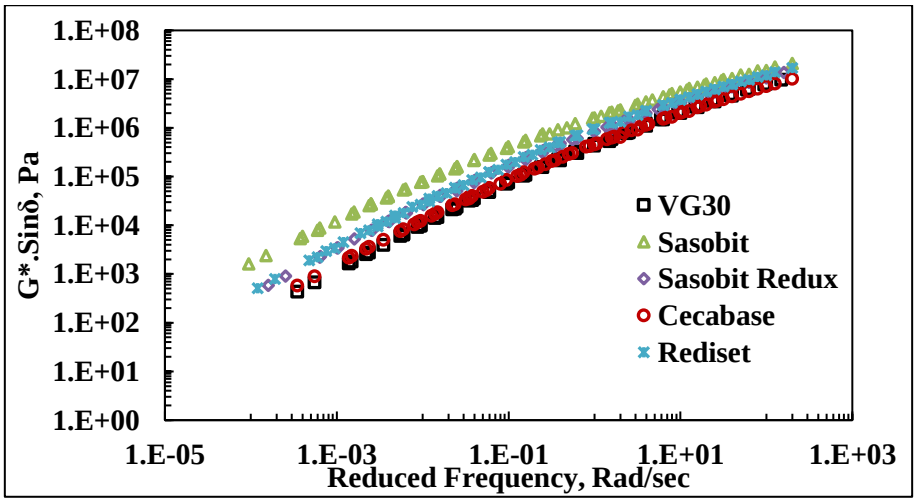

(b)

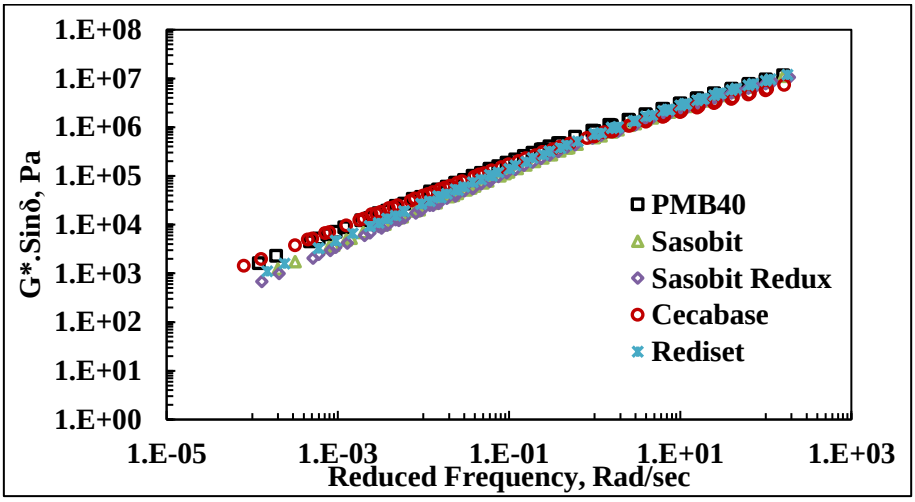


(c)

Figure 5.4. $|G^*|\sin\delta$ master curves at 20°C for different sample groups (a) GVG, (b) DVG, and (c) GP/DP

## 5.4 Rutting Performance

The MSCR test was conducted on STA samples using a 25 mm spindle and a 1 mm gap setting in the DSR following AASHTO T 350 [496]. Generally, two parameters, i.e., non-recoverable creep compliance ($J_{nr}$) and percentage recovery (%R), are calculated from the measured response in MSCR test. $J_{nr}$ is the ratio of unrecoverable strain to the applied stress, while %R is the percentage of recovered strain. The details about the test procedure and calculation of $J_{nr}$ & %R can be found elsewhere [10]. In the present study, MSCR test was carried out by applying four different stress levels (0.1, 3.2, 5, and 10 kPa) at four different test temperatures (40, 50, 60, and 70°C).

Figure (5.5-5.7) shows the variation in %R with the addition of WMA additives at different stress levels and test temperatures. As is apparent, there is a reduction in elastic response (%R) with the increase in stress levels and test temperatures. This is due to the inability of asphalt binder to restore the strain accumulated under high stresses and temperatures [253]. The reduction in %R with stress levels was more pronounced at

elevated temperatures. At highest test temperature (70°C in this study) and stress level (10 kPa), all the WMA binders (irrespective of WMA type and base asphalt binder) indicated negligible recovery values. For VG30 and PMB40, the addition of WMA additives showed either similar or improved %R. However, the extent of improvement depends on the combination of WMA type and base asphalt binder. For instance, despite the lower ageing temperature, inclusion of Rediset in VG30 (GR and DR combination) led to a similar elastic response as VG30, while its addition in PMB40 (GPR and DPR) resulted in higher %R than PMB40. Similar variations were observed for other combinations of WMA additives and base asphalt binders. This behavior inevitably varied with change in stress levels and test temperatures as well. Among different WMA additives, Sasobit indicated higher improvement with VG30, whereas Cecabase imparted superior elasticity with PMB40. This behavior was consistent at all the stress levels and test temperatures.

Figure (5.8-5.10) presents the variation in $J_{nr}$ values with the addition of WMA additives at different stress levels and test temperatures. The results indicated that $J_{nr}$ value increases rapidly with temperature (40-70°C). This is because the asphalt binder behaves as a viscous fluid at higher temperatures and thus indicated higher rutting susceptibility. Considering stress levels, the magnitude of $J_{nr}$ was found to increase gradually with the increase in stress from 0.1 kPa to 10 kPa. The probable reason for high $J_{nr}$ may be the shear thinning phenomenon of asphalt binder, which initiates at high-stress levels [498]. This implies that stress generated due to heavy vehicular loading led to higher rutting in the asphalt binder. It was found that the addition of WMA additives considerably influences the rutting behavior of base asphalt binders. The change may be negative or positive depending on the type of WMA additive and its interaction with the base asphalt binder. Due to the crystallization effect, Sasobit

imparted stiffness to the asphalt binder at the test temperatures, thereby showing excellent rutting performance [207]. This behavior was independent of base asphalt binder, stress level, and test temperature. Notably, at high temperatures and stress levels, all the WMA binders perform similar or even better than base asphalt binders. Attributable to the difference in interaction, the impact of WMA additives was observed to be more favorable for VG30 than PMB40.

An attempt has been made to compare the elastic response and non-recoverable creep compliance of WMA binders with their respective base asphalt binders. The comparison was made based on the line of equality approach, as shown in Figure 5.11. The equality line was plotted to elucidate the variation between WMA and base asphalt binders. The x-axis shows the $\%R/J_{nr}$ value of the base asphalt binder, while the value of $\%R/J_{nr}$ corresponding to WMA binders is displayed on y-axis. These values were independent of stress levels and test temperatures. For %R, a value above the line of equality is desirable, whereas a lower value for $J_{nr}$ is preferable for better rutting performance. As can be seen, all the WMA binders were near the line of equality. This clearly showed that the incorporation of WMA additives imparted similar to better elasticity with comparable (or even higher) rutting resistance than base asphalt binders. Based on Figure 5.11, it can be stated that reduced ageing temperatures did not influence the elastic nature or rutting behavior of WMA binders.

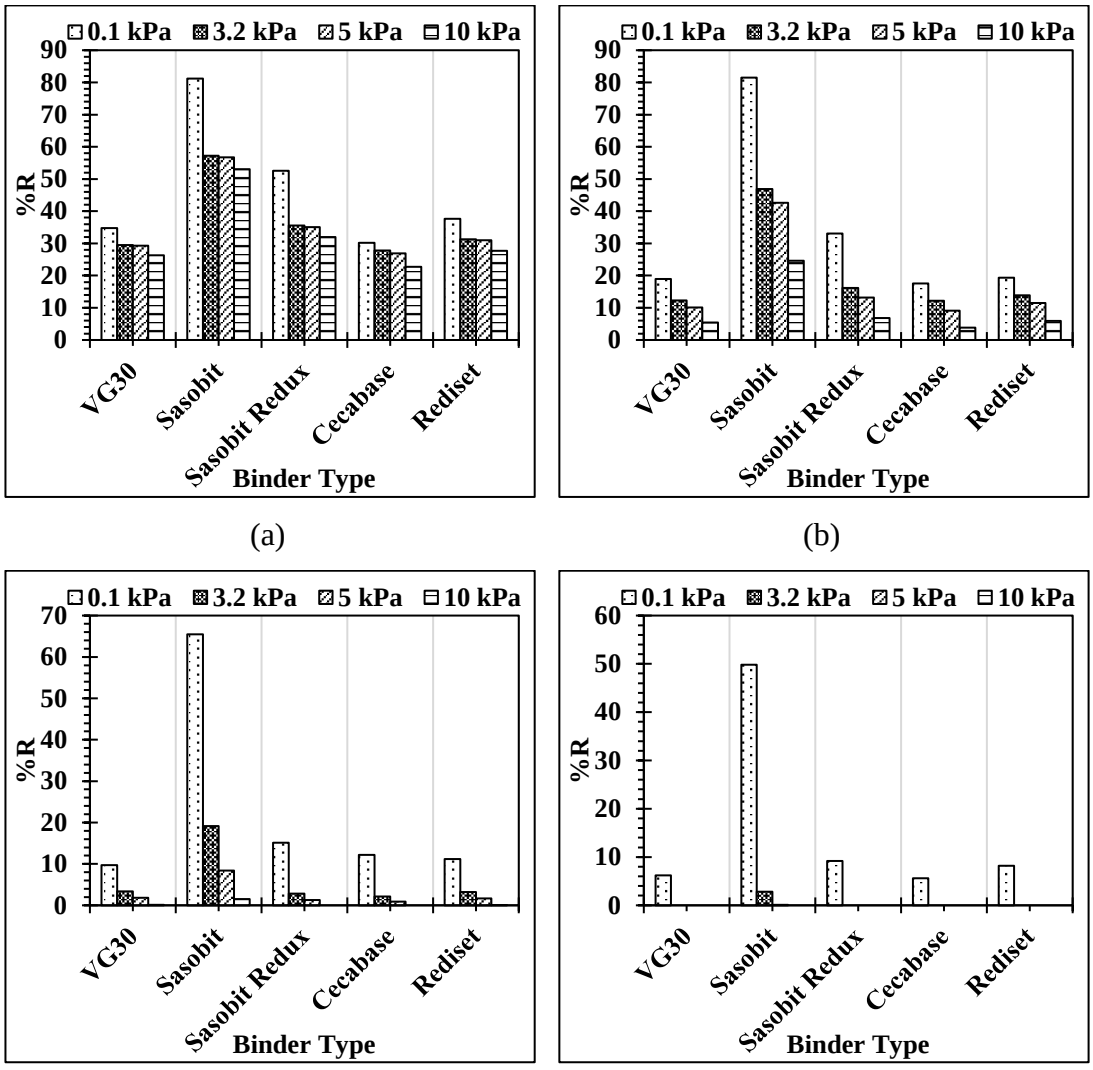


Figure 5.5. Percent recovery of WMA binders for GVG group at different temperatures (a) 40°C, (b) 50°C, (c) 60°C, and (d) 70°C

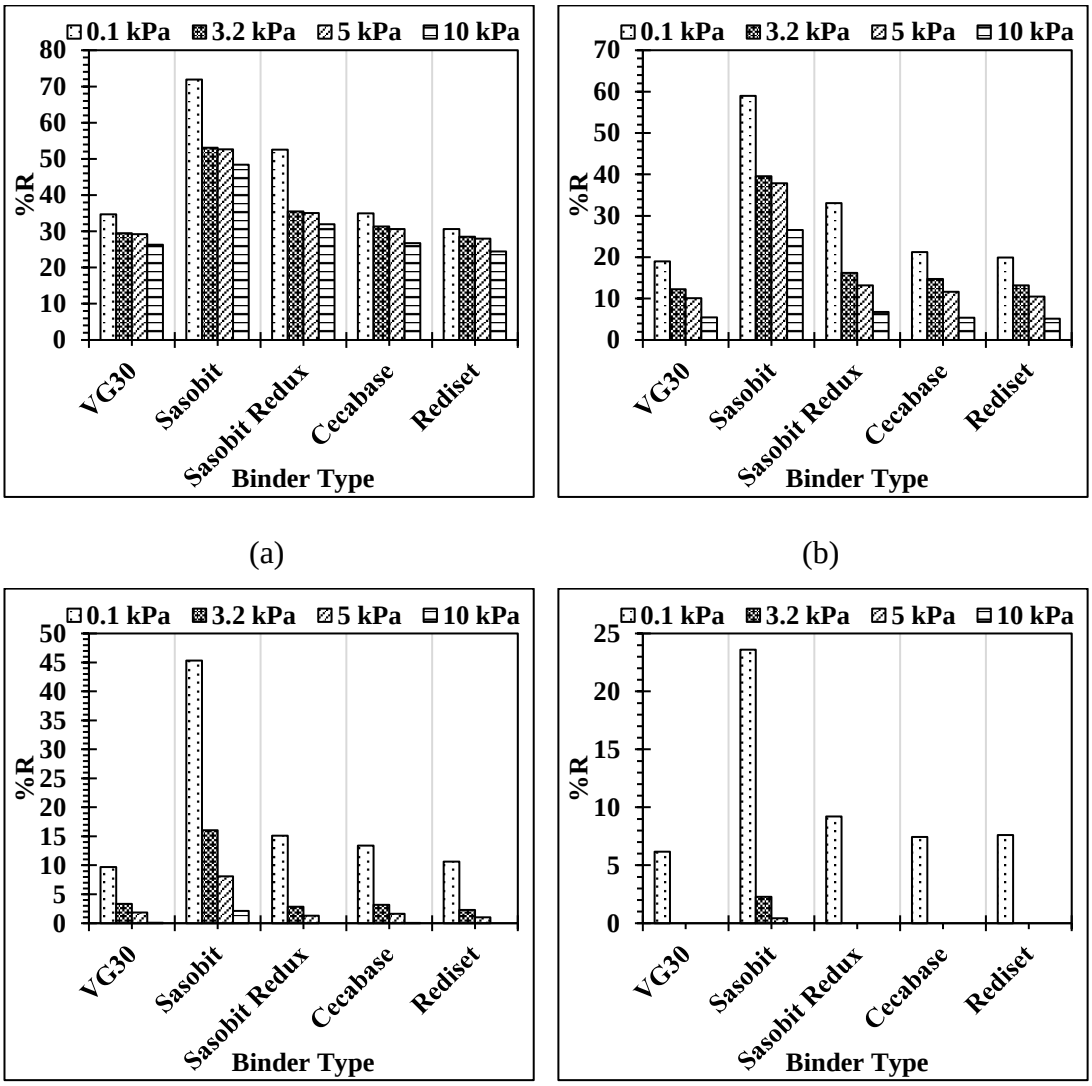


Figure 5.6. Percent recovery of WMA binders for DVG group at different temperatures (a) 40°C, (b) 50°C, (c) 60°C, and (d) 70°C

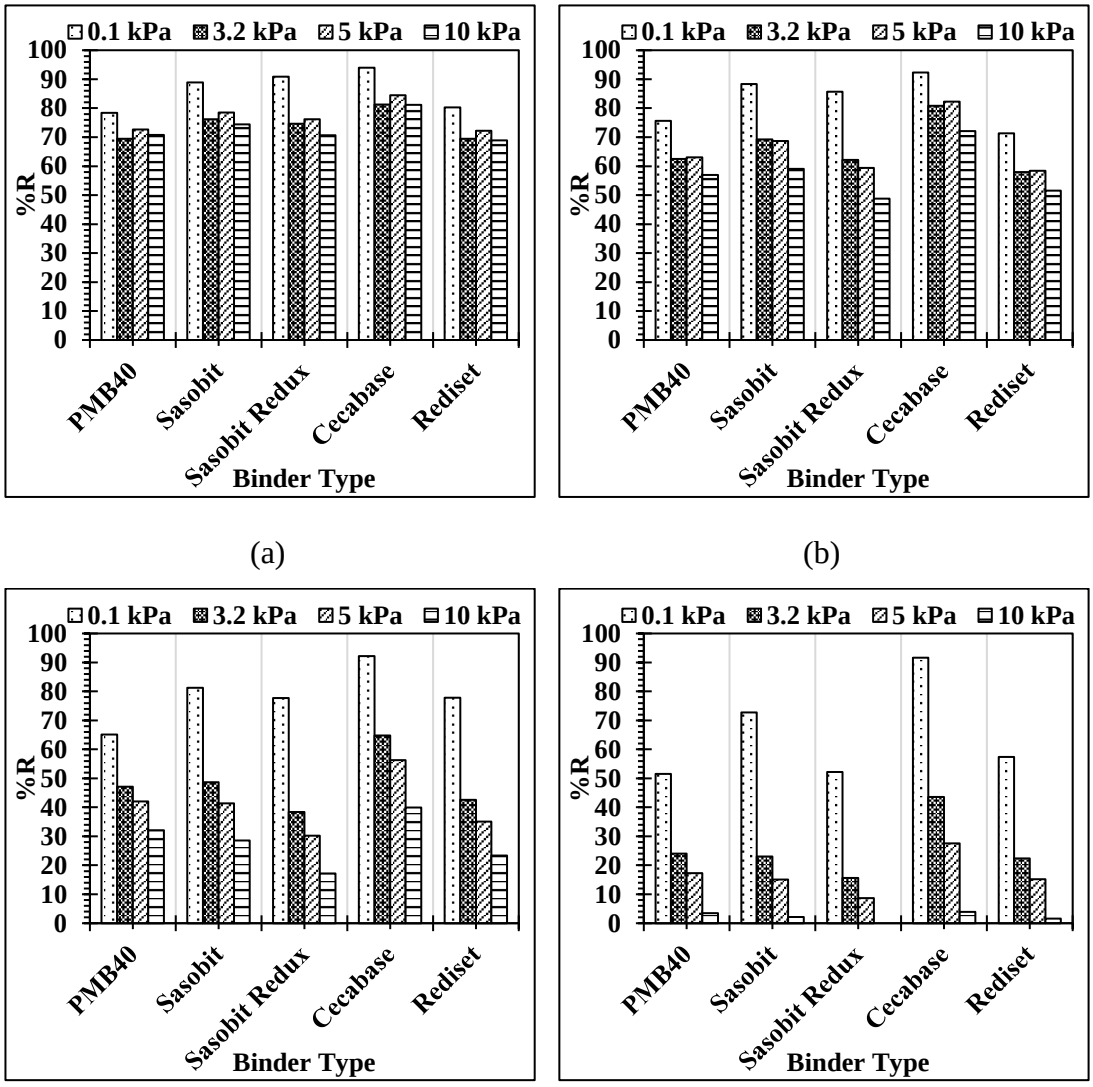


Figure 5.7. Percent recovery of WMA binders for GP/DP group at different temperatures (a) 40°C, (b) 50°C, (c) 60°C, and (d) 70°C

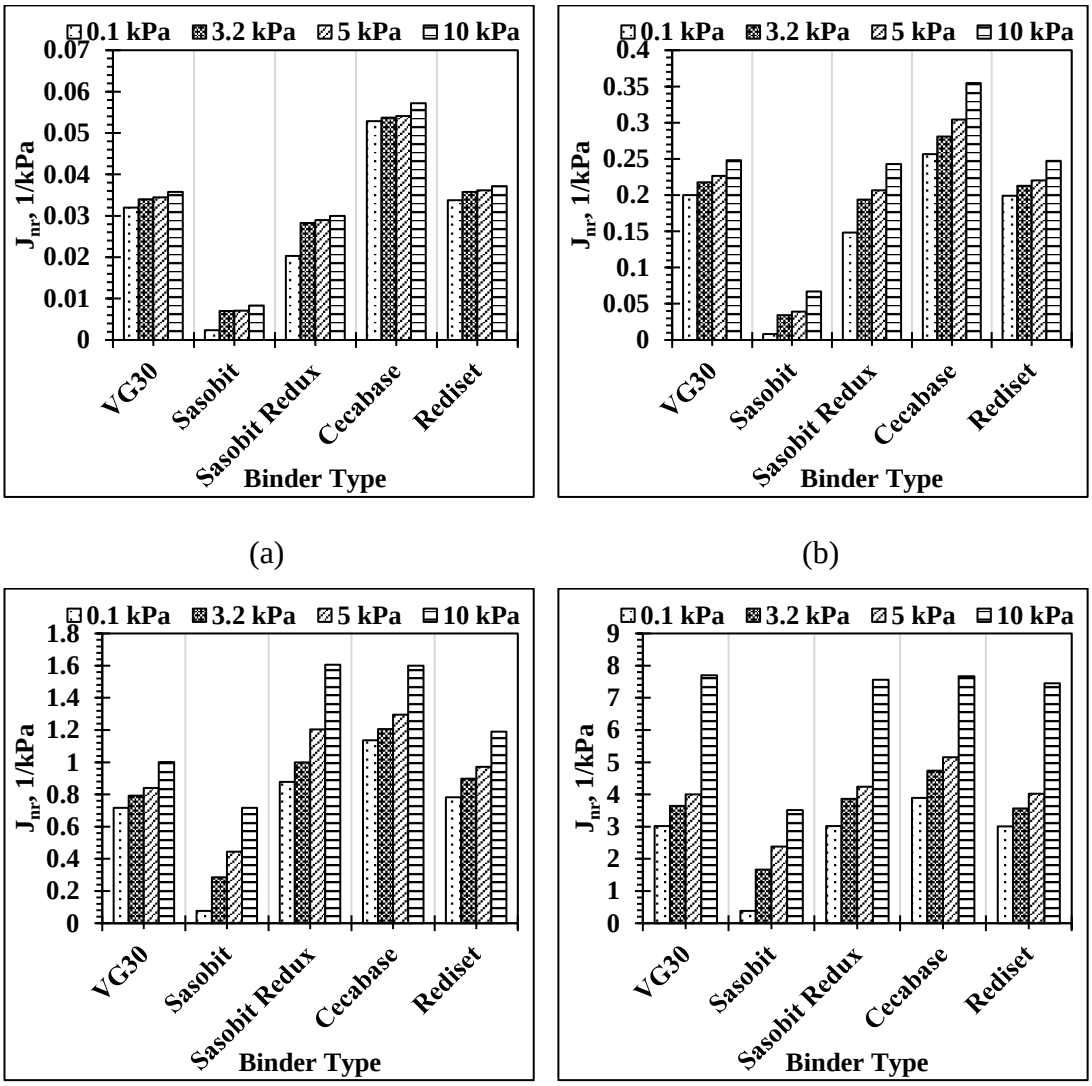


Figure 5.8. Non-recoverable creep compliance of WMA binders for GVG group at different temperatures (a) 40°C, (b) 50°C, (c) 60°C, and (d) 70°C

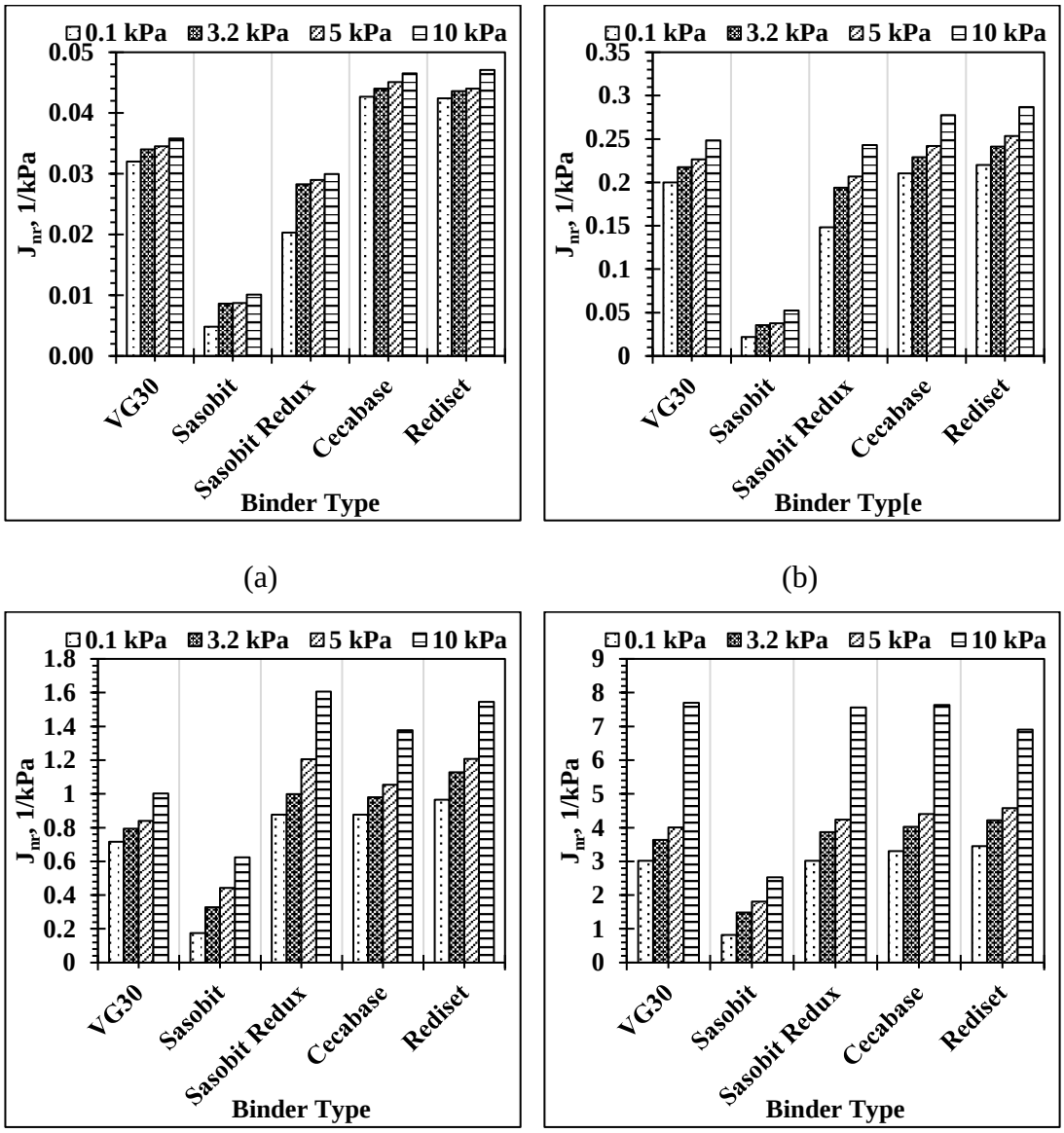


(a) (b)

(c) (d)

Figure 5.9. Non-recoverable creep compliance of WMA binders for DVG group at different temperatures (a) 40°C, (b) 50°C, (c) 60°C, and (d) 70°C

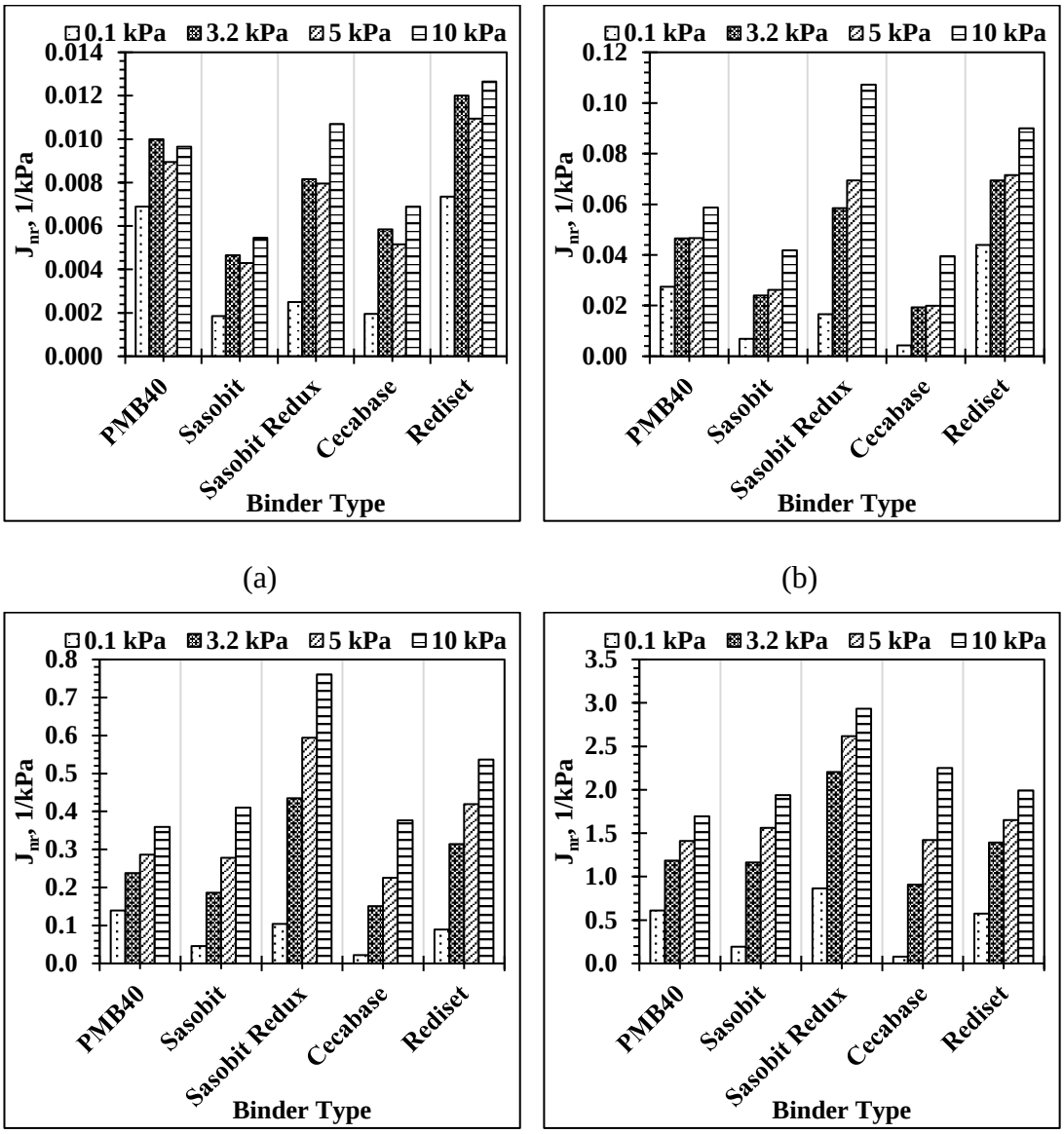


Figure 5.10. Non-recoverable creep compliance of WMA binders for GP/DP group at different temperatures (a) 40°C, (b) 50°C, (c) 60°C, and (d) 70°C

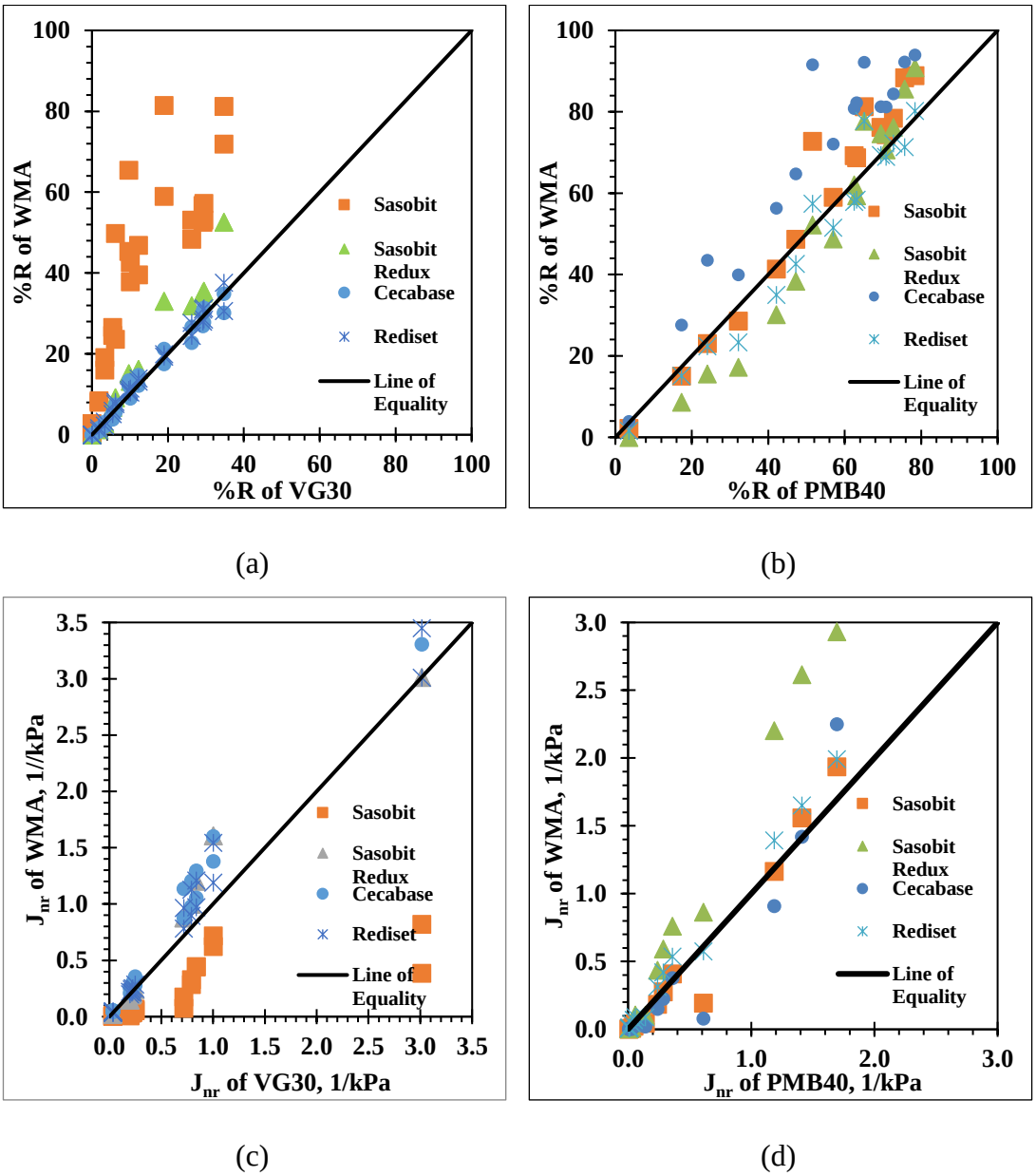


Figure 5.11. Comparison between all the considered asphalt binders based on MSCR parameters (a) %R for VG30, (b) %R for PMB40, (c) $J_{nr}$ for VG30, and (d) $J_{nr}$ for PMB40

### 5.4.1 Application of Arrhenius Equation

Since MSCR test was conducted at multiple stress levels and temperatures, a single parameter which combines the effect of temperature and stress levels, was chosen to rank the rutting resistance of asphalt binders. This parameter is

$\frac{\overline{E_a}}{\bar{J}_{nr\,(Maximum\,Temperature)} * \bar{m}}$ and the unit of the parameter is kPa. kJ/mol [552]. $\overline{E_a}$ is the average activation energy obtained by modelling the variation of $J_{nr}$ with temperature using an Arrhenius equation (Equation 5.3). $\bar{J}_{nr\,(Maximum\,Temperature)}$ is the average value of $J_{nr}$ obtained at the highest temperature, 70 °C in this study. $\bar{m}$ is the average value of stress sensitivity obtained by fitting a straight line between $J_{nr}$ and stress levels. The values of $\overline{E_a}$ and $\bar{J}_{nr\,(Maximum\,Temperature)}$ are averaged over stress levels while $\bar{m}$ is averaged over temperatures. The variation in $J_{nr}$ and model fittings are presented in Figure (5.12-5.14). As can be seen, Arrhenius equation can be appreciably applied to model the variation between $J_{nr}$ and 1/T. The applicability of Arrhenius model has been validated for different WMA binders at various stress levels. Mathematically, it can be written as:

$$J_{\mathrm{nr}} = Ae^{-\frac{E_{\mathrm{a}}}{RT}} \tag{5.3}$$

$$J_{nr,T_i} = P + m\sigma \tag{5.4}$$

In the above equations (Equations 5.3 and 5.4), $T$ is the absolute temperature in Kelvin, $E_{\mathrm{a}}$ is the activation energy, $R$ is the universal gas constant (8.314 J/mol.K), $\sigma$ is the stress and, $A$, $P$ and $m$ are model constants. The values of these parameters are not presented in detail for brevity. The information about the development and details of this parameter can be found elsewhere [552].

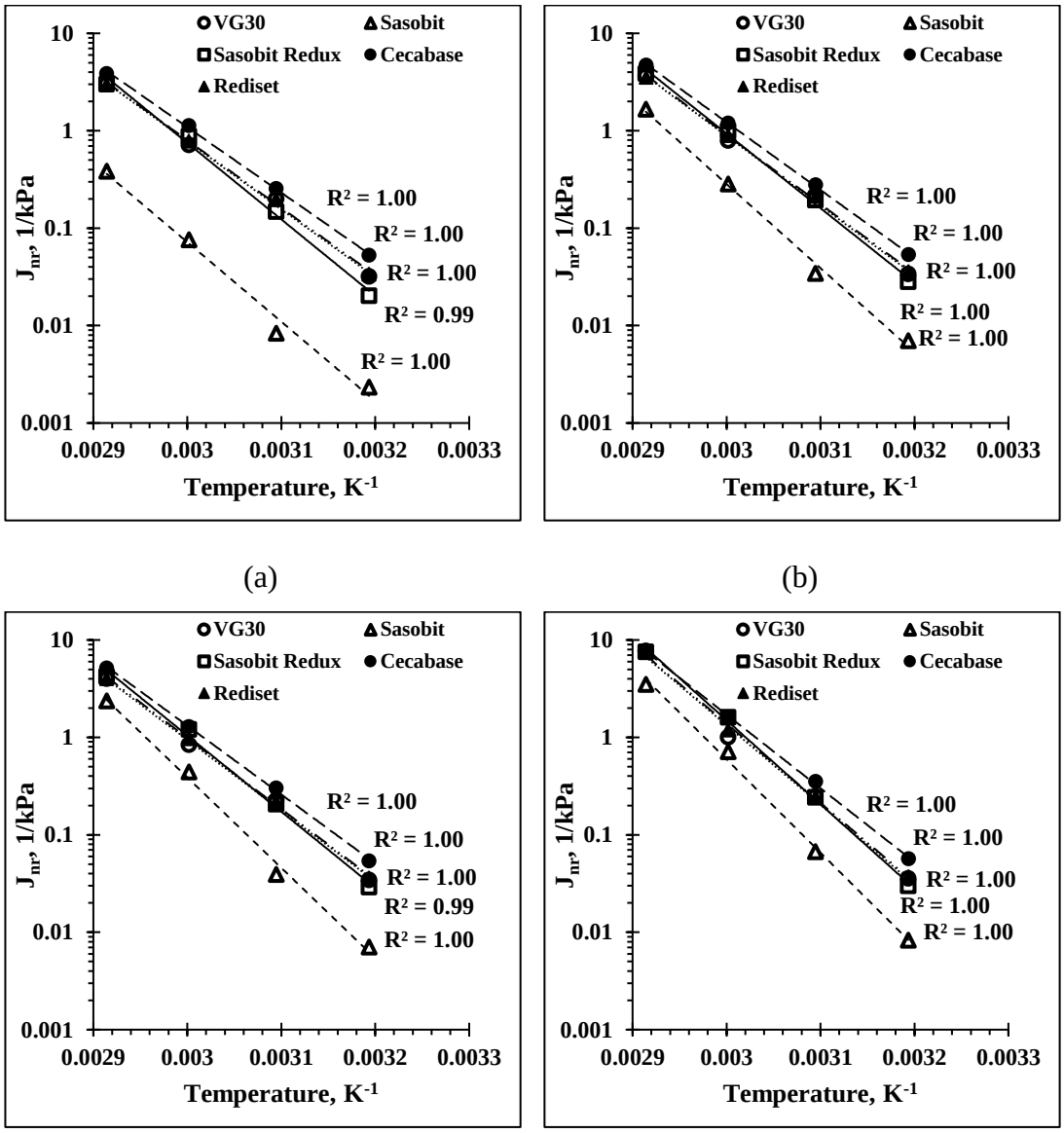


Figure 5.12. Validation of Arrhenius model for variation of Jnr versus 1/T for GVG group at (a) 0.1 kPa, (b) 3.2 kPa, (c) 5 kPa, and (d) 10 kPa

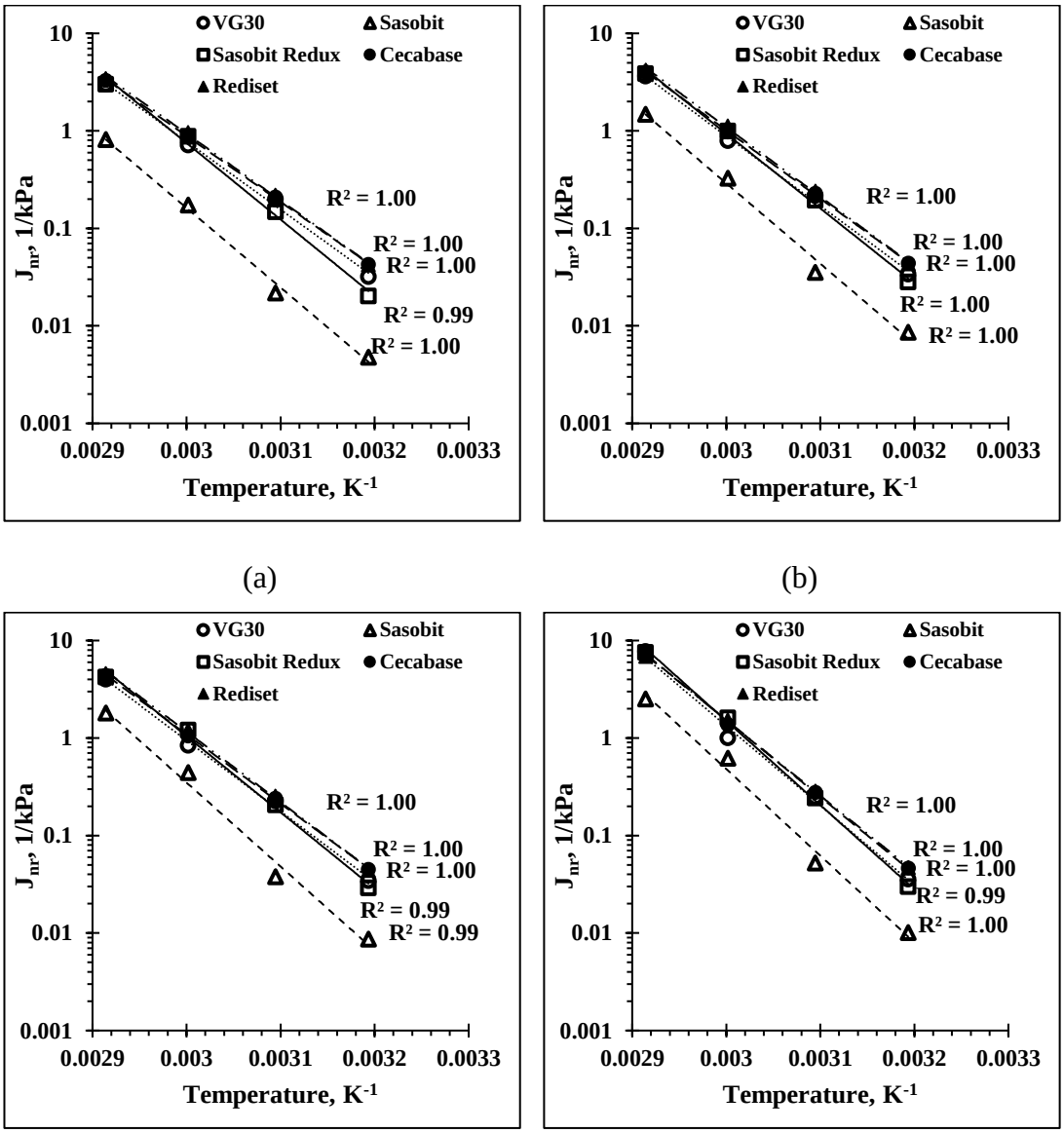


Figure 5.13. Validation of Arrhenius model for variation of $J_{nr}$ versus 1/T for DVG group at (a) 0.1 kPa, (b) 3.2 kPa, (c) 5 kPa, and (d) 10 kPa

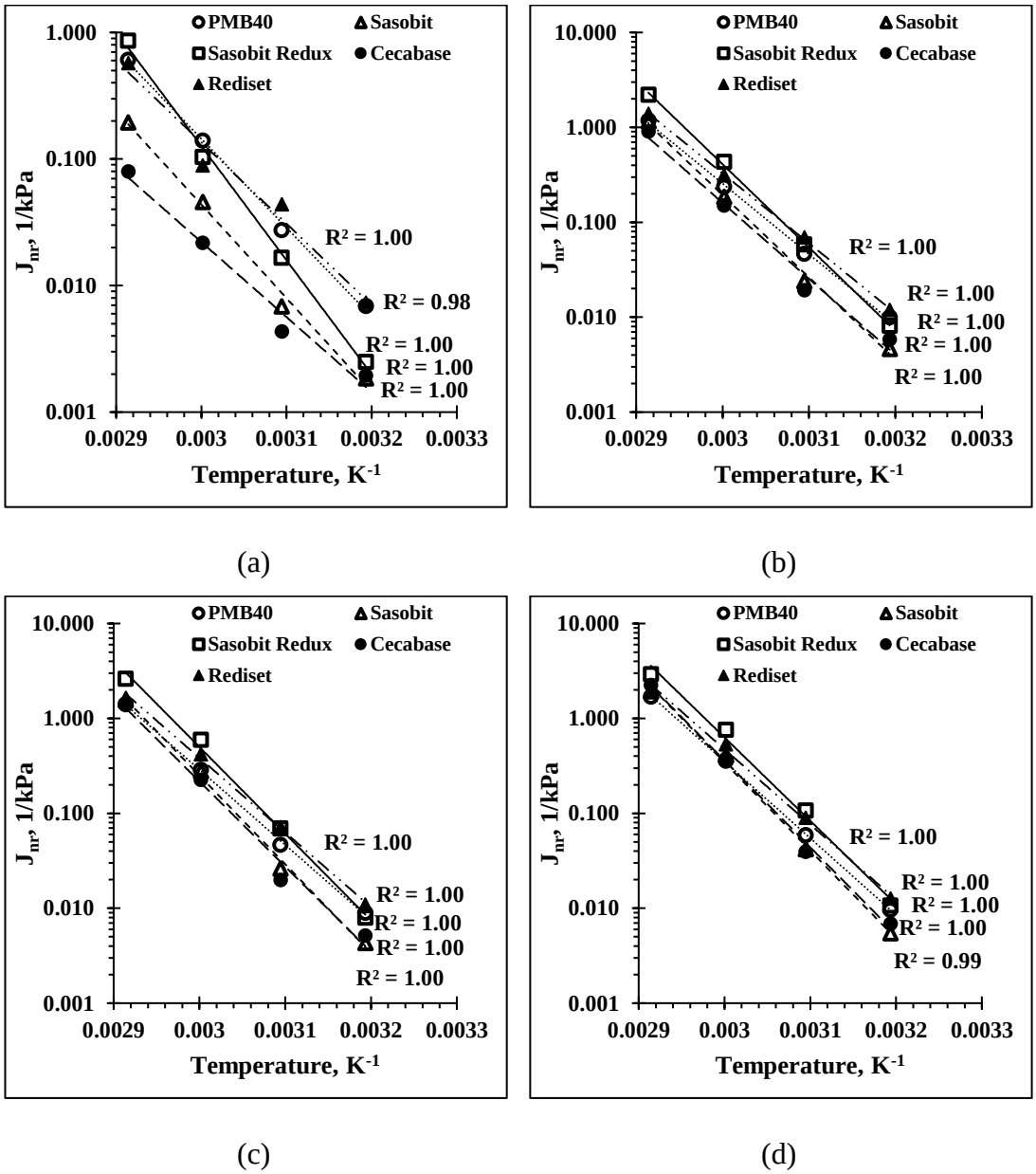


Figure 5.14. Validation of Arrhenius model for variation of $J_{nr}$ versus 1/T for GP/DP group at (a) 0.1 kPa, (b) 3.2 kPa, (c) 5 kPa, and (d) 10 kPa

Figure 5.15 (a-c) shows the value of rutting parameter (RP) and the effect of modification in terms of modification index (MI). MI is the ratio of RP value obtained after the addition of WMA additives and RP value of base asphalt binder. In order to determine the MI of WMA, the MI value of reference base asphalt binder was assumed to be unity. In general, higher $\frac{\overline{E_a}}{\bar{J}_{nr\,(Maximum\,Temperature)}*\bar{m}}$ or RP indicates better rutting

resistance. As is evident, the inclusion of WMA additives in VG30 (except Sasobit) exhibit comparable high temperature performance (MI ranged from 0.95 to 1.17). The addition of Sasobit, on the other hand, indicated superior performance, irrespective of the sample group (3.77 times for GVG and 7.53 times for DVG). This is attributed to the formation of crystalline lattice structure of Sasobit wax, which increases the stiffness at test temperatures and so the rutting resistance. However, the effect of WMA additives was observed to be insignificant with PMB40, as indicated by lower value of MI for all WMA binders. All the WMA binders (prepared with PMB40 as base binder) displayed lower value of RP, signifying their inadequacy to resist heavy traffic loading. The difference in RP values for VG30 and PMB40 may be attributed to the difference in interaction of WMA additive with their respective base asphalt binders. Since the chemical composition (especially the percentage of saturates, asphaltenes, resins, and aromatics (SARA)) of VG30 and PMB40 are different, it is very much justified that their interaction with any WMA additive will be influenced accordingly [468]. It may be possible that crosslinking polymeric chain facilitates lower interaction of WMA additive, thereby lowers the resistance to load. The mechanism behind the formation of polymeric network and their influence on asphalt binders has not been considered in the scope of the present study but requires further exploration. Needless to say, RP value of WMA binders (prepared with PMB40) was found to be higher than WMA binders prepared with VG30.

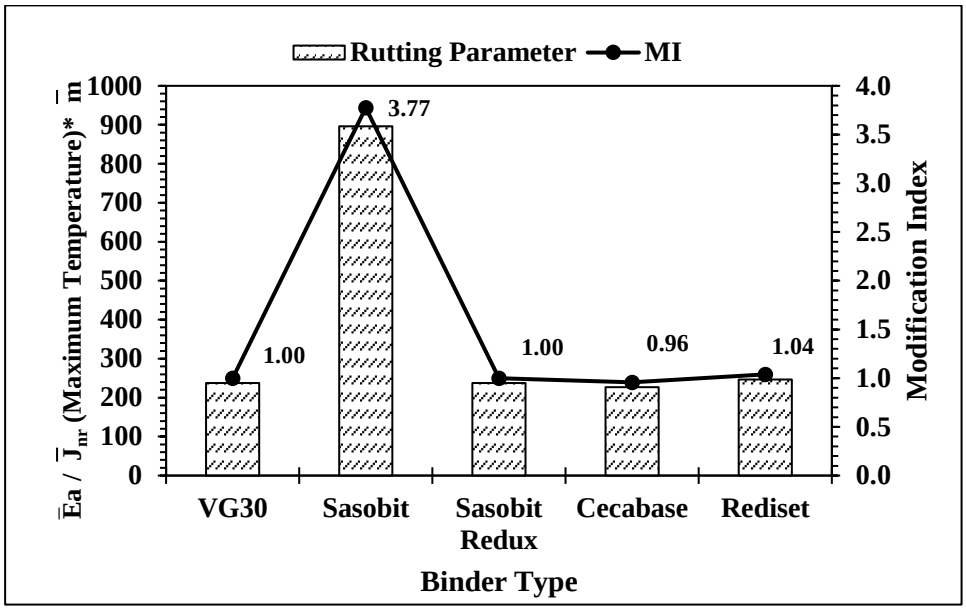
Rutting Parameter
MI
Ēa / J̄nr (Maximum Temperature)* m̄
Modification Index
1000
900
800
700
600
500
400
300
200
100
0
4.0
3.5
3.0
2.5
2.0
1.5
1.0
0.5
0.0
3.77
1.00
1.00
0.96
1.04
VG30
Sasobit
Sasobit Redux
Cecabase
Rediset
Binder Type

(a)

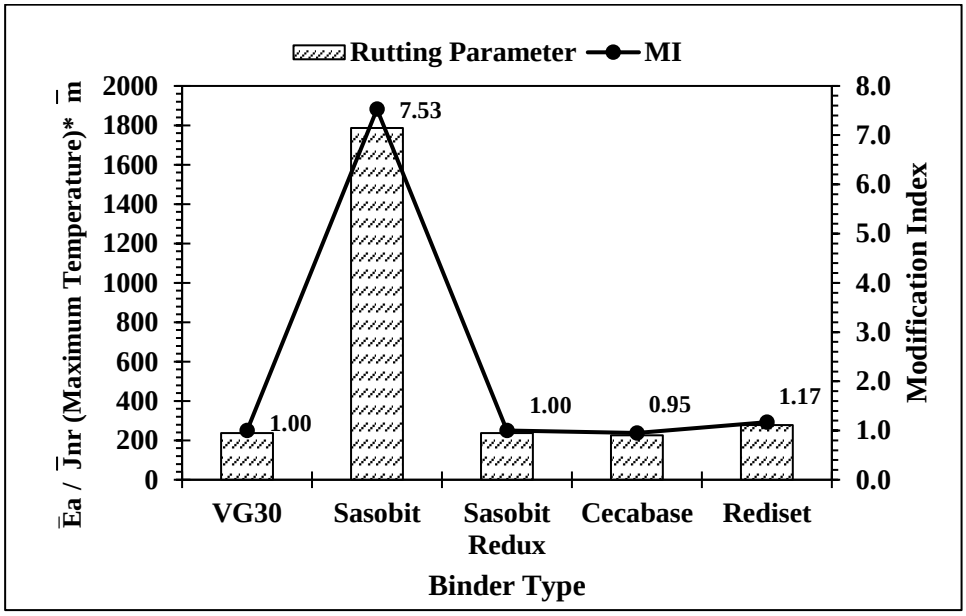
Rutting Parameter
MI
Ēa / J̄nr (Maximum Temperature)* m̄
Modification Index
2000
1800
1600
1400
1200
1000
800
600
400
200
0
8.0
7.0
6.0
5.0
4.0
3.0
2.0
1.0
0.0
7.53
1.00
1.00
0.95
1.17
VG30
Sasobit
Sasobit Redux
Cecabase
Rediset
Binder Type

(b)

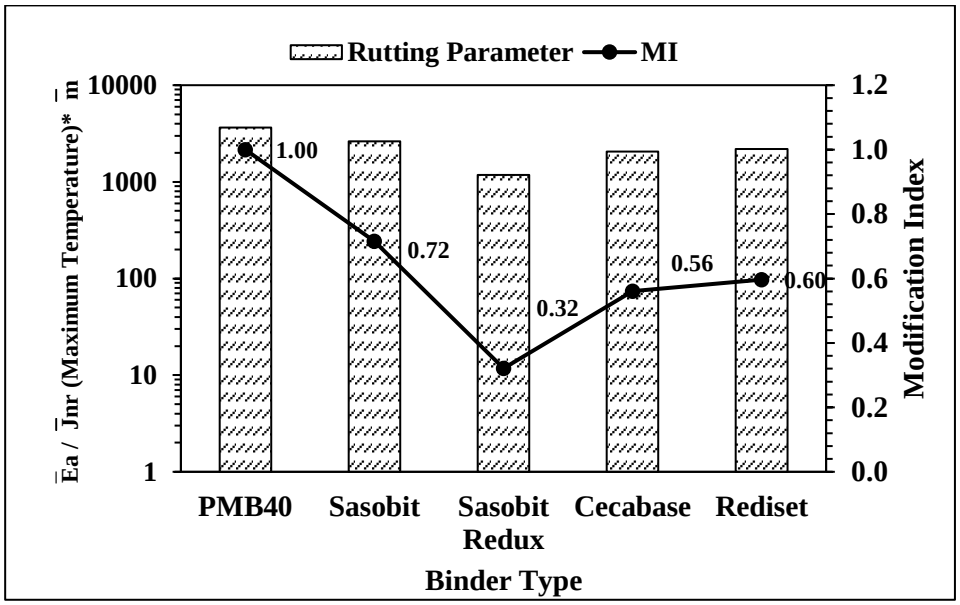


(c)

Figure 5.15. Rutting parameter and modification index for different sample groups (a) GVG, (b) DVG, and (c) GP/DP

## 5.5 Fatigue Performance

LAST was conducted as per the procedure outlined in AASHTO TP 101-14 [503]. LTA samples were utilized to perform the LAST using an 8 mm diameter spindle with a 2 mm gap setting in the DSR. LAST uses the VECD approach which originates from the concept of thermodynamics of irreversible process [553].

The generalized framework to explain the evolution of damage in asphalt binder is constructed using Equation 5.5 [554]

$$\frac{dD}{dt} = (-\frac{\partial W}{\partial D})^{\alpha} \tag{5.5}$$

$\alpha$ is the undamaged materials property and is calculated using the slope $m$ of the $|G^*|$ master curve (log-log plot), obtained during the frequency sweep in the LAST. $\alpha$ is the damage evolution rate parameter and can be calculated in two different ways, i.e.,

$1/m$ or $1 + 1/m$. [555] demonstrated that the damage characteristic curve (DCC) drawn by the use of 1/m is dependent on temperature and loading history, while DCC obtained by equating $\alpha$ to $1 + 1/m$ is independent of the temperature and loading (mode and amplitude). DCC describes the change in material integrity with an increase in damage. Hence, in this study, $1 + 1/m$ was used to calculate the value of $\alpha$. *W*, which is a representative of stored potential energy in the material, was quantified using the dissipated energy per cycle during the cyclic loading in DSR. Mathematically, it can be written as follows:

$$W = \pi {\gamma_p}^2 |G^*| \sin \delta \tag{5.6}$$

Equation 5.6 is derived by mathematically integrating the strain energy per unit volume, i.e. $\int \tau \mathrm{d}\gamma$ from an interval of 0 to $2\pi/\omega$. $\tau$ is the stress response for the input strain amplitude.

*D* in Equation 5.5 is the damage intensity of the asphalt binder, which is obtained by substituting Equation 5.6 in Equation 5.5 and numerically integrating the resultant [556]:

$$D(t) \cong \sum_{i=1}^{N} \left[\pi I_D {\gamma_p}^2 (|G^*| \sin\delta_{i-1} - |G^*| \sin\delta_i)\right]^{\frac{\alpha}{1+\alpha}} (t_i - t_{i-1})^{\frac{1}{1+\alpha}} \tag{5.7}$$

Where $I_D$ is an initial undamaged dynamic shear modulus (in MPa) divided by a modulus of 1 MPa.

The variation of $|G^*| \sin\delta$ with *D(t)* can be fitted using the following power law. The curve so obtained is the damage characteristic curve (DCC).

$$|G^*| \sin\delta = C_0 - C_1 (D)^{C_2} \tag{5.8}$$

where, $C_0$, $C_1$ and $C_2$ are model constants obtained through fitting the experimental data. Usually, $|G^*|\sin\delta$ is normalized and $C_0$ is taken as 1. Equations 5.5, 5.6, 5.7, and 5.8 are used to derive the following relationship between $N_f$ and $\gamma_p$.

$$N_f = \frac{f\left(D_f\right)^k}{k(\pi C_1 C_2)^\alpha}(\gamma_p)^{-2\alpha} \tag{5.9}$$

Where $f$ is the frequency during the test (10 Hz), $D_f$ represents the accumulated damage at failure, calculated using Equation 5.7. In the conventional LAST, failure is defined corresponding to peak stress obtained during the amplitude sweep test. k in Equation 5.9 is equal to 1 + (1-$C_2$)$\alpha$. Equation 5.9 is further simplified to generate a close form solution as given in Equation 5.10, where, $A = \frac{f(D_f)^k}{k(\pi C_1 C_2)^\alpha}$ and $B = -2\alpha$.

$$N_f = A\gamma^B \tag{5.10}$$

$N_f$ represents the number of cycles to failure for the a'sphalt binder. $A$ is a function of damage, while $B$ is undamaged material property. A high value of $A$ and a lower value of $B$ are desirable for improved fatigue life [557,558].

### 5.5.1 Stress-Strain Response of Asphalt Binders

The evolution of stress versus strain in the amplitude sweep phase of LAST can be used as an essential tool to understand the strain dependency and damage tolerance of asphalt binders during shear loading. These phenomenological indications (strain and damage tolerance) are usually interpreted based on the profile of the stress-strain curve. A sharper curve represents a higher strain dependency (lower fatigue resistance) of the asphalt binder, whereas a wider peak (higher fatigue resistance) implies a reduced dependency of asphalt binder on the applied strain [557]. A typical representation of

stress-strain curves (at three different temperatures) are shown in Figure 5.16. As can be seen, the stress value increased with the applied strain and reached a peak value. Beyond the peak point (defined as peak stress), the curve starts to decrease at a particular rate, indicating damage initiation and propagation within the asphalt binder. The strain value corresponding to the peak stress is defined as the failure strain (damage initiation). With the increase in temperature, peak stress reduced, while the corresponding failure strain increased (Figure 5.16). The reduction in peak stress is due to the reduced stiffness of asphalt binder and the higher failure strain indicates the enhancement in strain tolerance with the rise in test temperature. Similar trends were observed for all the WMA binders. However, their peak stress and corresponding failure strain varied depending on the type of WMA technology and base asphalt binder.

Figure (5.17-5.19) illustrates the stress-strain response for different combinations of WMA binders. It is worth noting that the addition of WMA additives in VG30, irrespective of their type, resulted in a relatively wider peak. On the other hand, all the WMA binders prepared with PMB40 exhibited opposite behavior, indicating sharper peaks in comparison to the peak profile of PMB40. This difference in the influence of WMA additives with the change in base asphalt binder was consistent at all the test temperatures (10, 20, and 30°C). Table 5.2 shows the value of peak stress and corresponding failure strain obtained using stress-strain response for different combinations of asphalt binders. It could be inferred that the inclusion of WMA additives in VG30 improved the strain tolerance (higher strain value) even at higher peak stress. With the dominance of polymeric network in PMB40, the effect of WMA binders was not very significant. Combination of WMA additives and PMB40 resulted in lower failure strain (except Cecabase) compared to PMB40 (without WMA additive), implying an adverse effect of WMA on the fatigue behavior. On an average, organic

additives improved the peak stress, whereas higher failure strain was evident with chemical agents. The higher peak stress indicates higher stiffness of the asphalt binders which is attributed to the presence of long chain hydrocarbon in organic waxes; on the other hand, the emulsifying effect of chemical agents might be the probable reason for improvement in failure strain [268,559,560]. Figure 5.20 shows the comparison between different WMA binders with respective to their respective base asphalt binders. A majority of data points were either coinciding or above the equality line; thus, it can be stated that the use of WMA additives may imparts satisfactory damage tolerance during shear loading. Since the asphalt binder exhibit viscoelastic behavior, it is very challenging to estimate the accurate fatigue performance merely based on the stress-strain response, rather it provides an idea to differentiate the extent of failure in terms of strain value.

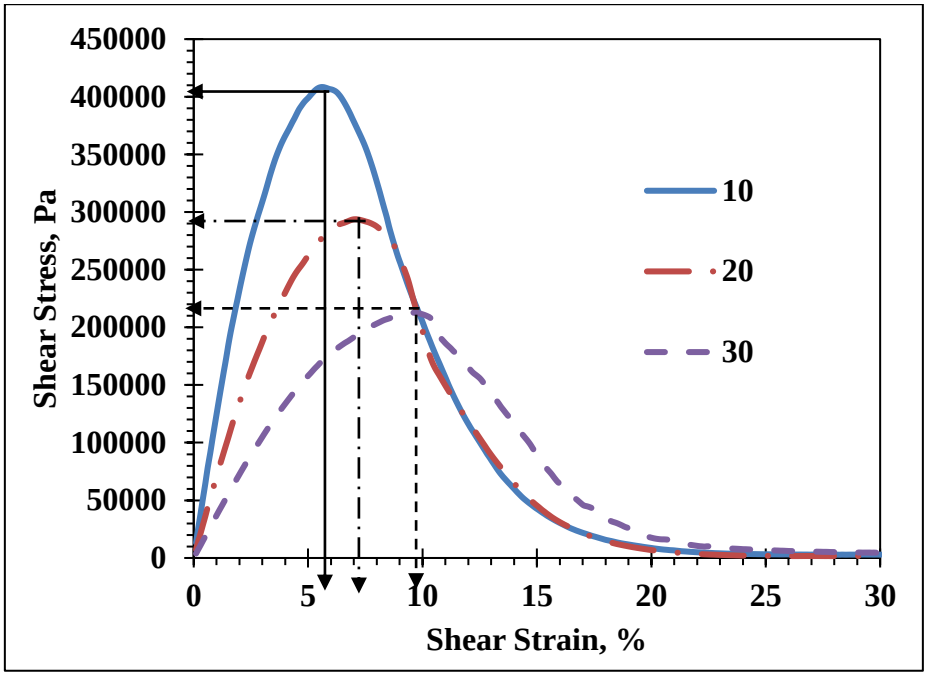


Figure 5.16. Variation in shear stress and shear strain with change in temperature

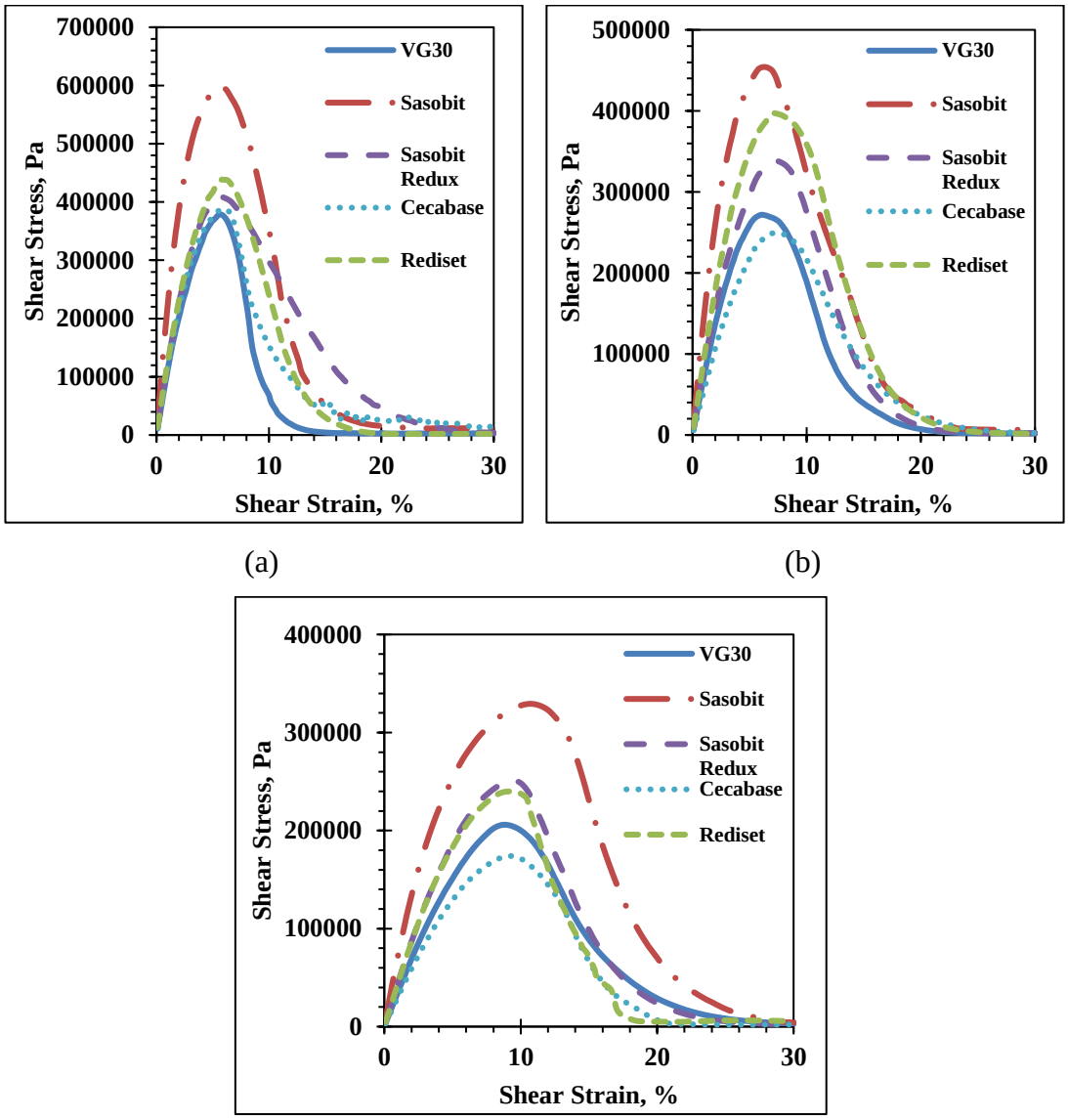


Figure 5.17. Shear stress amplitude of samples in GVG group as a function of shear strain at (a) 10°C, (b) 20°C, and (c) 30°C

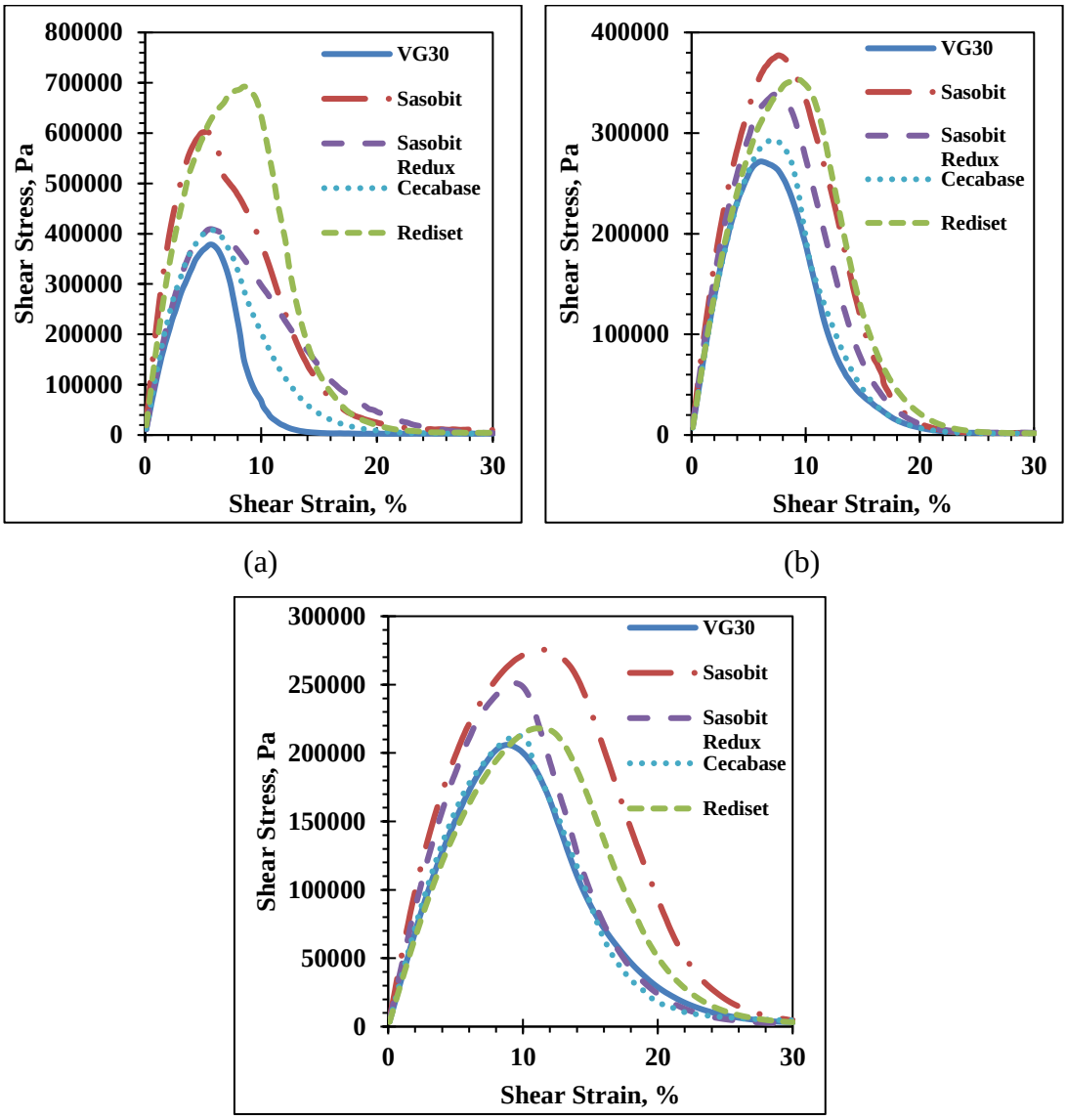


Figure 5.18. Shear stress amplitude of samples in DVG group as a function of shear strain at (a) 10°C, (b) 20°C, and (c) 30°C

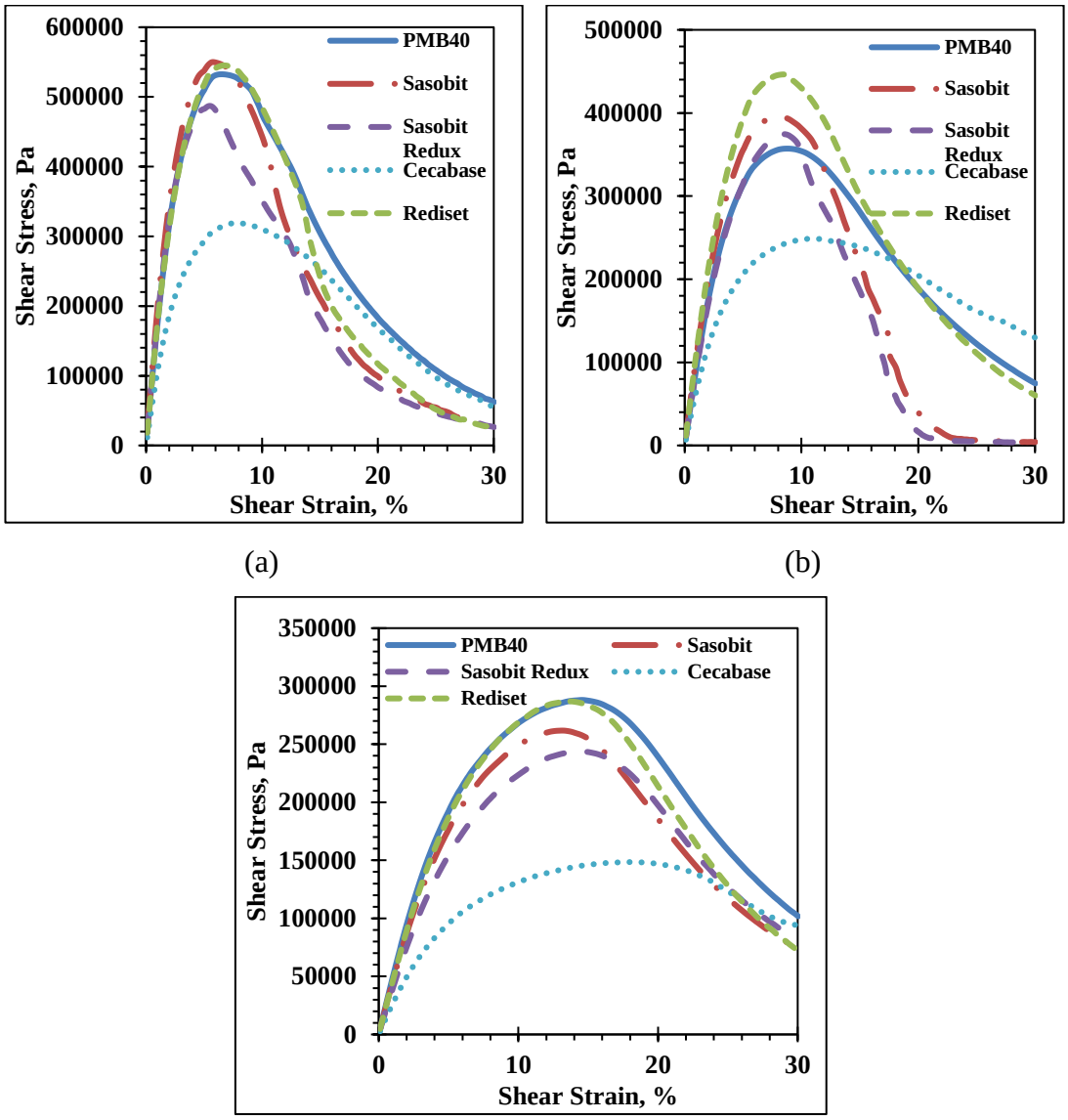


Figure 5.19. Shear stress amplitude of samples in GP/DP group as a function of shear strain at (a) 10°C, (b) 20°C, and (c) 30°C

Table 5.2. Peak stress and failure strain for different asphalt binders at different test temperatures

| Sample Group | Asphalt Binders | Peak Stress, Pa | | | Failure Strain, % | | |
|---|---|---|---|---|---|---|---|
| | | 10°C | 20°C | 30°C | 10°C | 20°C | 30°C |
| GVG | VG30 | 378574 | 271779 | 205955 | 5.64 | 6.14 | 8.84 |
| | Sasobit | 599251 | 454159 | 329282 | 5.63 | 6.23 | 10.73 |
| | Sasobit Redux | 409189 | 338351 | 251151 | 5.63 | 7.34 | 9.44 |
| | Cecabase | 388617 | 249425 | 174064 | 5.98 | 7.53 | 9.34 |
| | Rediset | 438521 | 397187 | 239965 | 5.84 | 7.14 | 9.23 |
| DVG | VG30 | 378574 | 271779 | 205955 | 5.64 | 6.14 | 8.84 |
| | Sasobit | 603023 | 377330 | 277882 | 5.32 | 7.64 | 11.58 |
| | Sasobit Redux | 409189 | 338351 | 251151 | 5.63 | 7.34 | 9.44 |
| | Cecabase | 409585 | 305223 | 212798 | 5.83 | 7.44 | 9.54 |
| | Rediset | 692399 | 357192 | 219537 | 8.54 | 9.19 | 11.19 |
| GP/DP | PMB40 | 532621 | 358281 | 288433 | 6.58 | 8.73 | 14.38 |
| | Sasobit | 550652 | 399406 | 261941 | 5.93 | 7.93 | 12.98 |
| | Sasobit Redux | 511785 | 374573 | 244627 | 5.97 | 8.43 | 14.33 |
| | Cecabase | 326035 | 248849 | 149019 | 8.83 | 11.04 | 17.58 |
| | Rediset | 552817 | 446650 | 289214 | 6.83 | 8.43 | 13.43 |

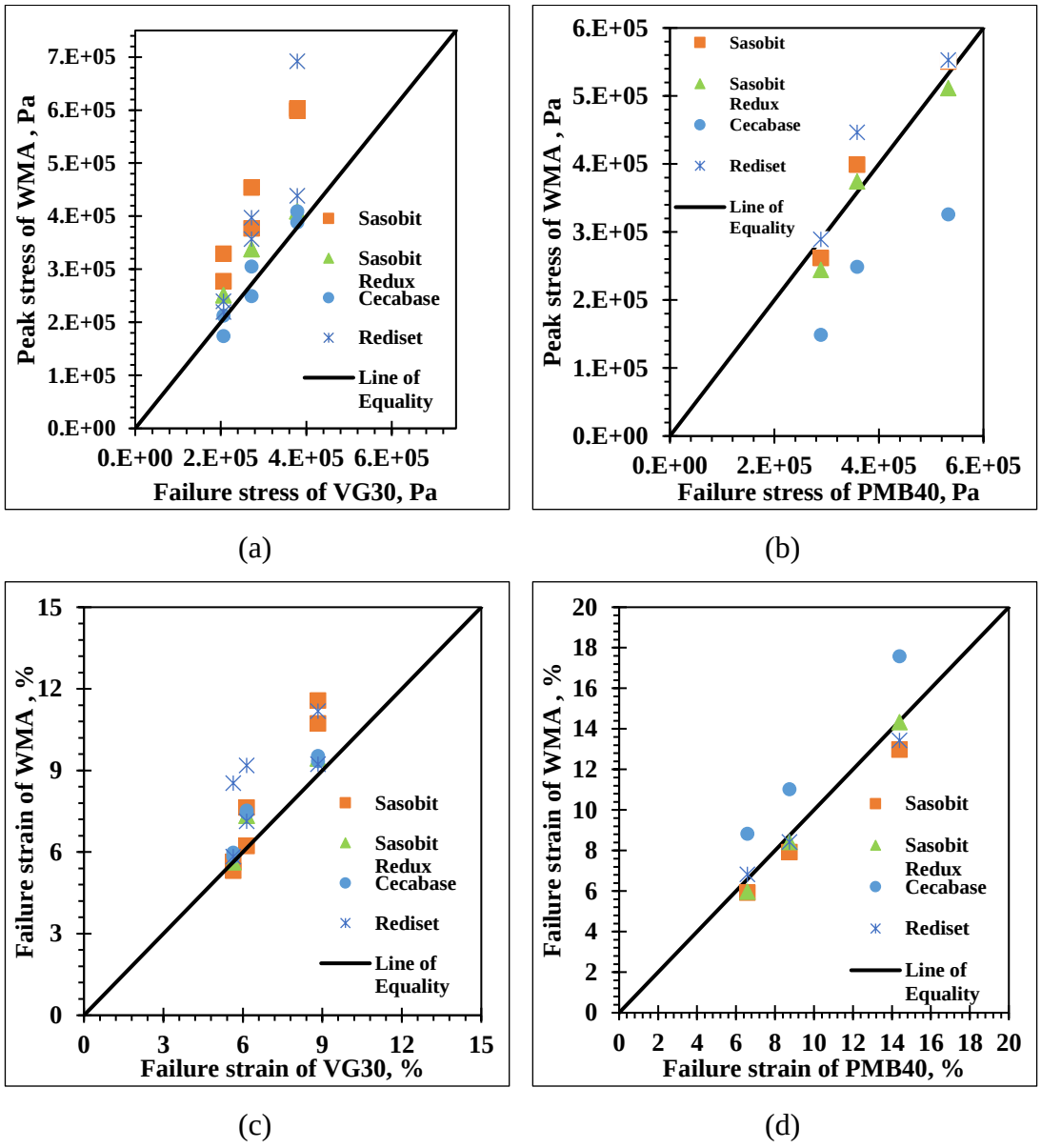


Figure 5.20. Comparison between all the considered asphalt binders based on their stress-strain response (a) Peak stress for VG30, (b) Peak stress for PMB40, (c) Failure strain for VG30, and (d) Failure strain for PMB40

### 5.5.2 Fatigue Life of Asphalt Binders

Fatigue life, in general, varies with the change in temperature and strain amplitude. An increase in temperature and strain amplitude resulted in lower fatigue life, as shown in Figure 5.21. The extent and rate of reduction with an increase in strain amplitude depends on the magnitude of fatigue parameters, such as *A* and *B*. The magnitudes of *A*

and *B* (−2α) are used to study the fatigue behavior of asphalt binders using a LAST, where *A* is a function of damage, and *B* indicates the undamaged material property. The value of *A* increased while the magnitude of *B* decreased with the increase in temperature, indicating an improvement in fatigue resistance. However, no specific trend was observed in *A* and *B* with the change in WMA additive. Irrespective of the test temperatures, value of *A* for WMA binders (prepared with VG30) was observed to be higher than VG30. This indicates the positive impact of WMA over the damage characteristics at intermediate test temperatures (10, 20, and 30°C). In the case of PMB40, the positive impact was only evident for Cecabase (a chemical-based WMA agent). Interestingly, the influence of WMA on the value of *B* was not very significant. On average, chemical-based WMA binders showed a lower *B* value, indicating improved strain susceptibility, whereas organic-based WMA binders displayed higher strain susceptibility (higher *B* value). This difference is clearly visible from the fatigue life ($N_F$) plots shown in Figure (5.22-5.24).

As is evident, the value of $N_F$ varied significantly with strain amplitudes. However, the variation in $N_F$ is a function of temperature, WMA additive, and base asphalt binder. Chemical-based WMA binders (Rediset in VG30 and Cecabase in PMB40) displayed superior fatigue performance throughout the strain amplitudes. This observation was consistent at all the test temperatures (10, 20, and 30°C). With strain amplitudes, a steep reduction in $N_F$ was observed for Sasobit-modified asphalt binders. At lower strain amplitudes, the addition of Sasobit in VG30 leads to higher $N_F$, irrespective of the test temperature. As the strain increases (beyond 8-10%), the fatigue curve declined and coincided with VG30. The variation in $N_F$ with strain is attributed to higher *B* value of Sasobit-modified asphalt binder (Table 5.3), signifying higher strain susceptibility. This behavior was not evident in PMB40; instead, the combination (GPS and DPS) displayed

comparable fatigue performance at intermediate temperatures. It is worth noting that even though the addition of Sasobit imparted higher stiffness (as described by $|G^*|\sin\delta$) and strain susceptibility (higher *B*), its impact on the fatigue life was satisfactory. Sasobit Redux, another organic-based WMA binder, performed similar to their respective base asphalt binder. Overall, it can be stated that WMA binders does not deteriorate the fatigue performance of asphalt binders, irrespective of test temperature and base asphalt binder.

Table 5.3. Fatigue parameters and fatigue life equation for all the tested asphalt binders at different test temperatures

| **Sample Group** | **Asphalt Binders** | **Fatigue Life, $N_F = A(\gamma)^B$** | | |
|---|---|---|---|---|
| | | **10°C** | **20°C** | **30°C** |
| **GVG** | **VG30** | $607994(\gamma)^{-5.16}$ | $1376292(\gamma)^{-5.07}$ | $5985794(\gamma)^{-4.85}$ |
| | **Sasobit** | $3461291(\gamma)^{-5.84}$ | $4861769(\gamma)^{-5.67}$ | $58936034(\gamma)^{-5.31}$ |
| | **Sasobit Redux** | $1734938(\gamma)^{-5.56}$ | $4423171(\gamma)^{-5.19}$ | $8900931(\gamma)^{-4.84}$ |
| | **Cecabase** | $1402400(\gamma)^{-5.28}$ | $4080784(\gamma)^{-4.96}$ | $8717989(\gamma)^{-4.87}$ |
| | **Rediset** | $1049825(\gamma)^{-5.25}$ | $4584188(\gamma)^{-5.21}$ | $8789112(\gamma)^{-4.95}$ |
| **DVG** | **VG30** | $607994(\gamma)^{-5.16}$ | $1376292(\gamma)^{-5.07}$ | $5985794(\gamma)^{-4.85}$ |
| | **Sasobit** | $1838084(\gamma)^{-5.77}$ | $6055229(\gamma)^{-5.20}$ | $59207471(\gamma)^{-5.11}$ |
| | **Sasobit Redux** | $1734938(\gamma)^{-5.56}$ | $4423171(\gamma)^{-5.19}$ | $8900931(\gamma)^{-4.84}$ |
| | **Cecabase** | $1595781(\gamma)^{-5.28}$ | $4330468(\gamma)^{-5.04}$ | $9395183(\gamma)^{-4.84}$ |
| | **Rediset** | $14284543(\gamma)^{-5.36}$ | $10860838(\gamma)^{-5.05}$ | $20748635(\gamma)^{-4.81}$ |

| | | | | |
|---|---|---|---|---|
| GP/DP | **PMB40** | 19919050 $(\gamma)^{-5.93}$ | 74949121$(\gamma)^{-5.65}$ | 370210294$(\gamma)^{-5.27}$ |
| | **Sasobit** | 5411793$(\gamma)^{-5.77}$ | 17159063$(\gamma)^{-5.44}$ | 128266650$(\gamma)^{-5.09}$ |
| | **Sasobit Redux** | 14210400$(\gamma)^{-5.79}$ | 21289608$(\gamma)^{-5.48}$ | 237928473$(\gamma)^{-5.15}$ |
| | **Cecabase** | 184692321$(\gamma)^{-5.86}$ | 321807262$(\gamma)^{-5.67}$ | 958351354$(\gamma)^{-5.27}$ |
| | **Rediset** | 12483204$(\gamma)^{-5.66}$ | 29210020$(\gamma)^{-5.39}$ | 149820071$(\gamma)^{-5.06}$ |

*Note: $\gamma$ indicates stain corresponding to peak stress. A and B are LAST damage and undamaged parameters, respectively.*

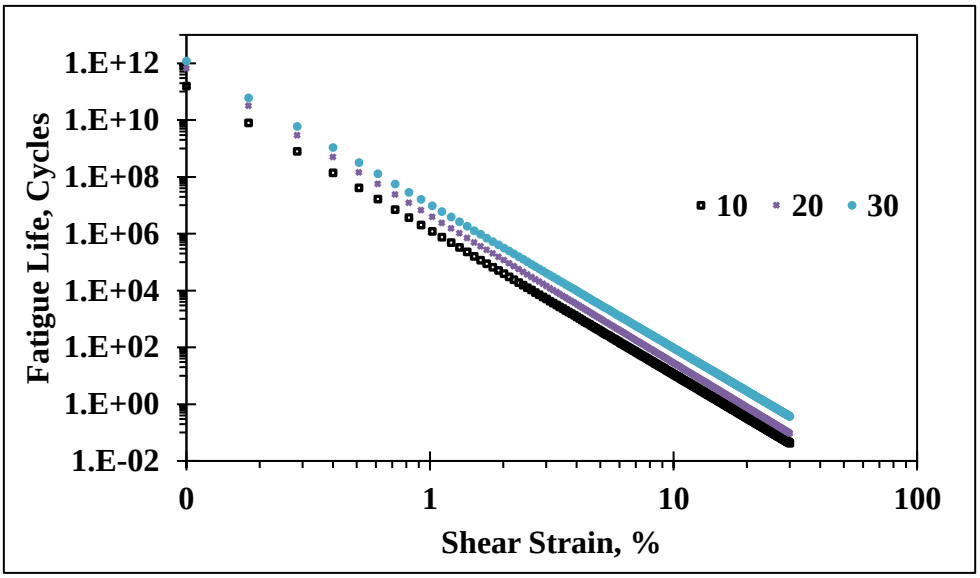


Figure 5.21. Schematic representation of $N_F$ with strain amplitudes at different temperatures

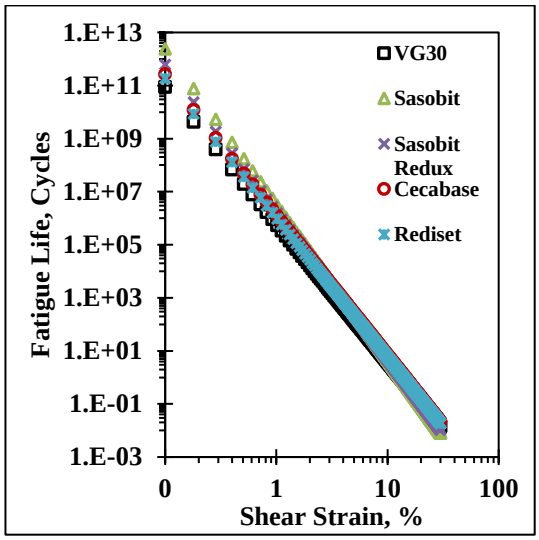


(a)

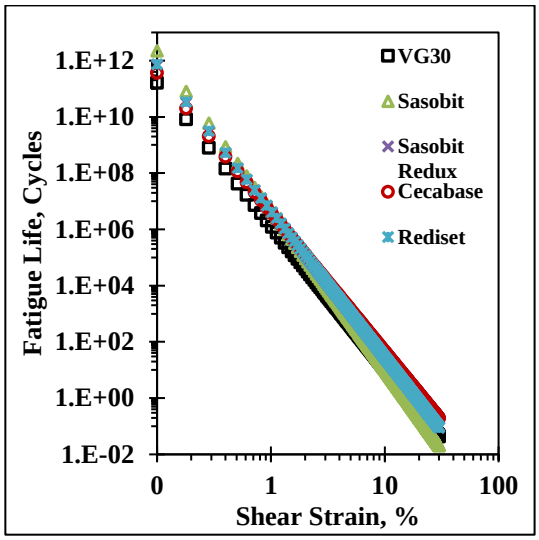


(b)

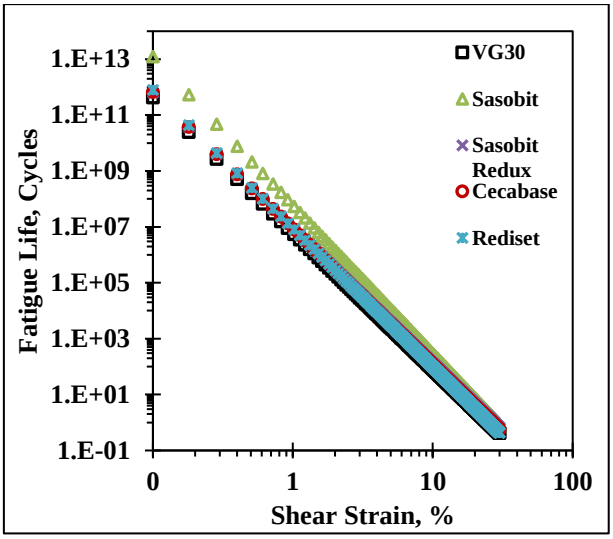


(c)

Figure 5.22. $N_F$ of samples in GVG group as a function of strain amplitude at (a) 10°C, (b) 20°C, and (c) 30°C

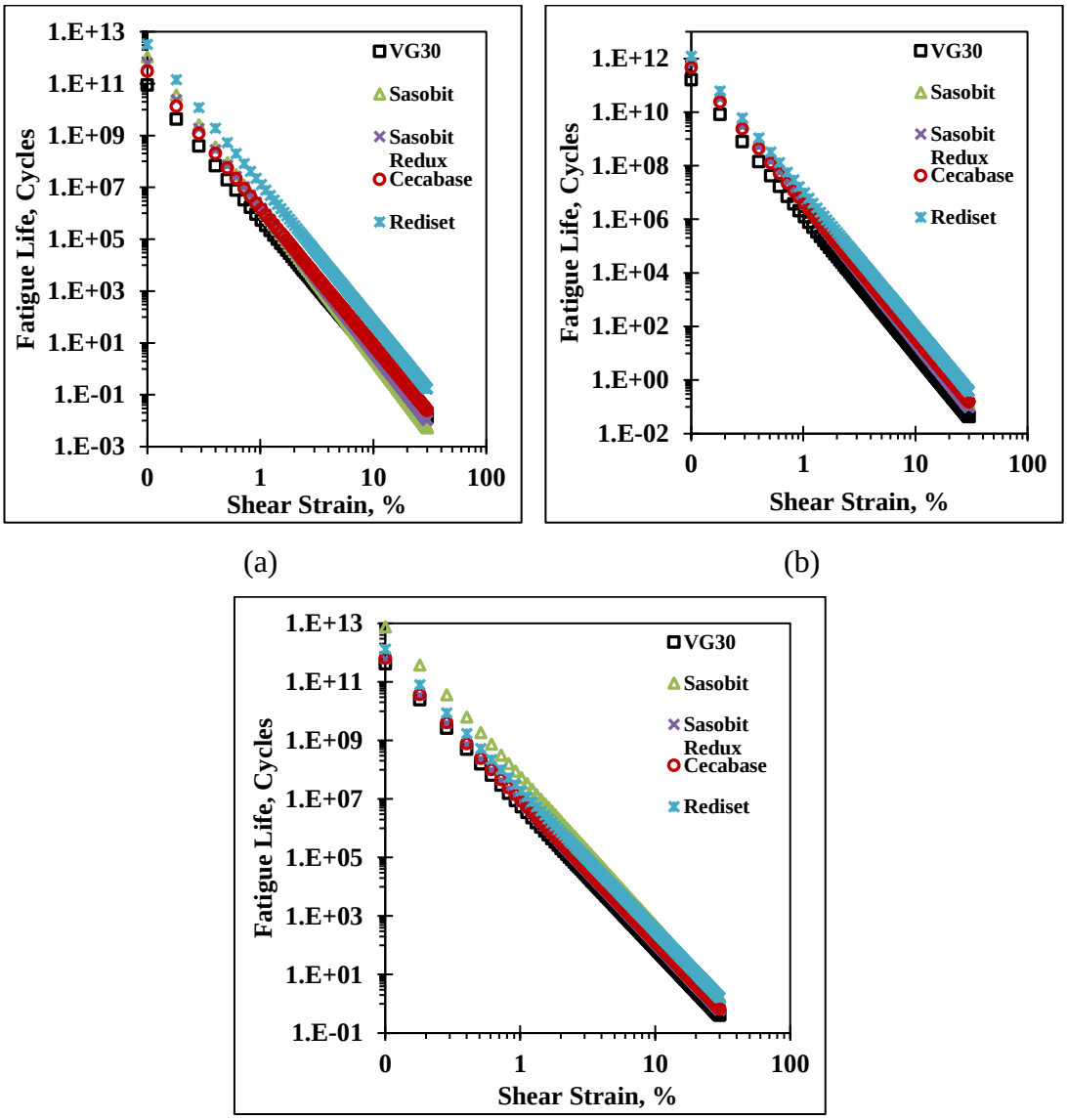


Figure 5.23. $N_F$ of samples in DVG group as a function of strain amplitude at (a) 10°C, (b) 20°C, and (c) 30°C

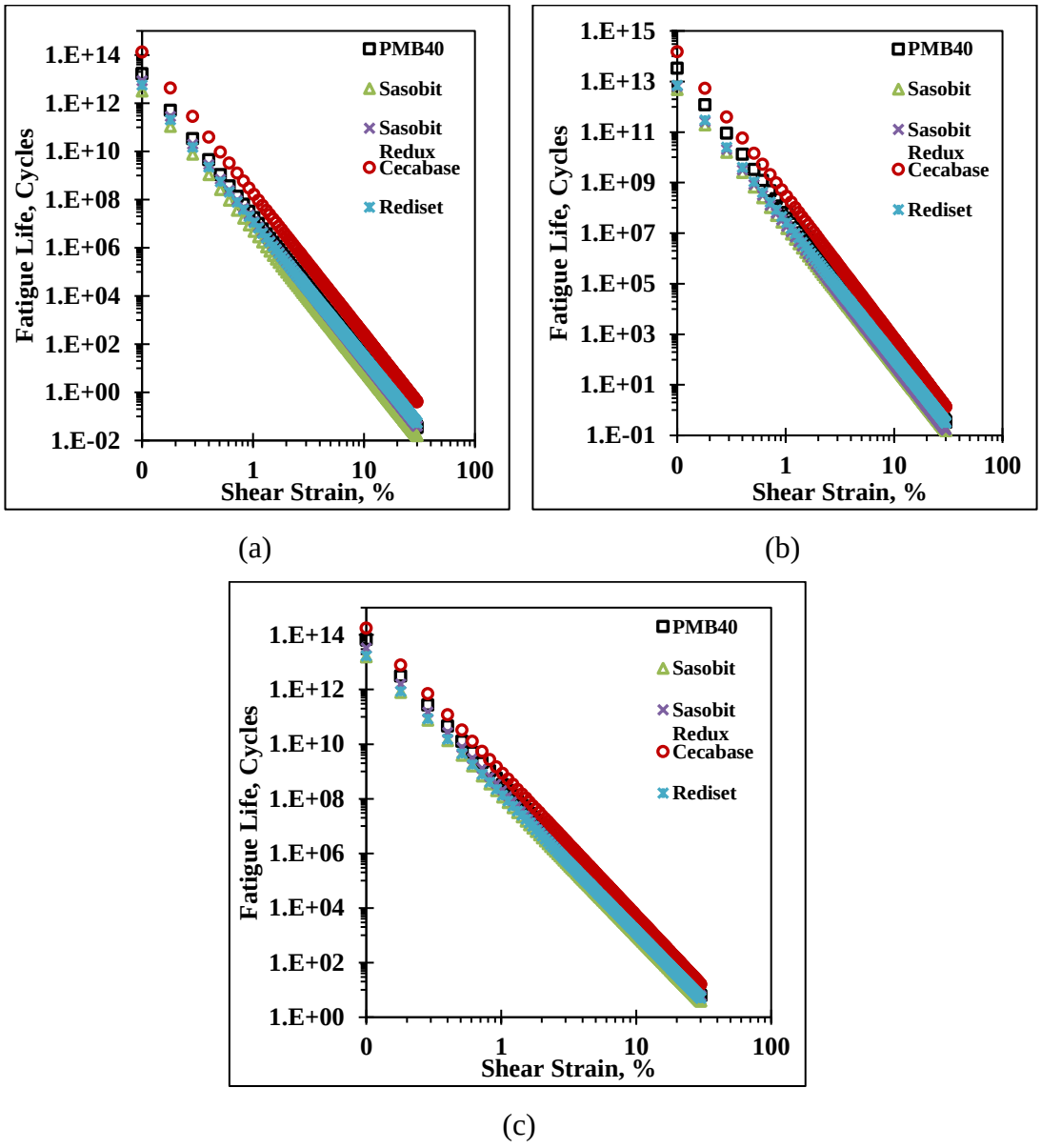


Figure 5.24. $N_F$ of samples in GP/DP group as a function of strain amplitude at (a) 10°C, (b) 20°C, and (c) 30°C

## 5.6 Moisture Resistance

Moisture damage has been identified as a major concern for asphalt pavements. Asphalt binder, in an asphalt mix, holds the mineral aggregates together and acts as an adhesive sealant against moisture. Various mechanisms have been proposed to explain the occurrence of moisture damage [561]. Broadly, ingress of moisture in an asphalt

mixture lead to the occurrence of cohesive failure (failure within the asphalt binder) and/or adhesive failure (bond failure between asphalt binder and aggregate) [562,563]. Identification of these failure modes in an asphalt mixture is crucial to understand the compatibility between aggregate and asphalt binder, and to assess the effect of asphalt binder modification, if any, on the strength characteristics of the asphalt binder. Water ingression often breaks the adhesive bond between the asphalt binders and aggregates, resulting in the separation/removal of the asphalt binder from the aggregate surface [564]. This phenomenon is generally referred to as stripping (or adhesive failure). In cohesive failure, though the bond between the aggregate and bitumen is not broken, the thickness of asphalt binder film reduces due to failure within the bitumen structure [565,566]. The failure may further accelerate by the continuous movement of vehicles over the pavement, as shown in Figure 5.25. Suction by tire threads pulls out moisture from the surface and within the asphalt mixture. This pulling force on the asphalt binder film increases the chances of adhesive failure as shown in Figure 5.25b.

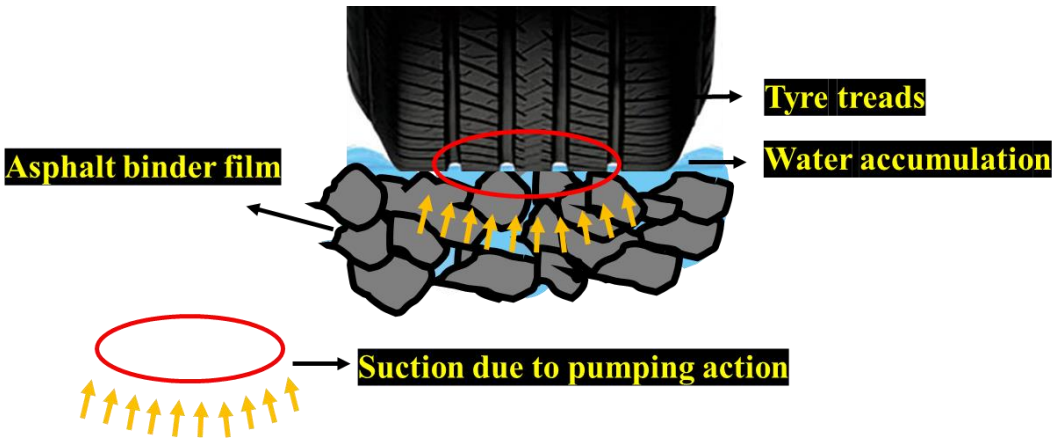


(a)

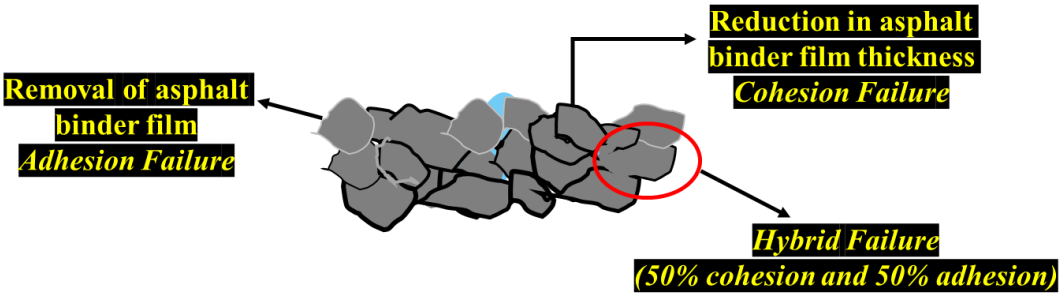


(b)

Figure 5.25. Bond strength mechanism (a) Effect of wheel passage during the rainy season and (b) Bond failure due to the combined action of wheel pass and moisture

In addition to the individual material properties and interaction between them, the production temperature of asphalt mixture also influences its performance against moisture [105]. During production, aggregate and binder are heated to high temperatures, which removes any residual moisture from the surface of the aggregates and facilitates improved BS [325,339]. There is a belief that technologies which aid in the production of asphalt mixtures at lower temperatures in comparison to hot mix asphalt, for example, WMA, may lead to improper drying of aggregates and will increase the susceptibility of the mix to moisture attack. While several studies [277,284,289,304,323,567] have demonstrated that performance of WMA (produced using different technologies) in terms of rutting and fatigue characteristics are comparable to (or even better than) HMA, performance in terms of moisture resistance has not been explored to a satisfactory extent. Results on moisture resistance of WMA, considering the effect of base binder (use to prepare WMA), aggregate type, and test methods used for quantification of moisture damage, are not available. Therefore, there is a need to study the effect of lower production temperatures on the moisture resistance of WMA and compare its results with the response of conventional HMA.

Figure 5.26 (a-d) presents the influence of WMA additives on the BS values of different asphalt binder – aggregate combinations in dry and wet conditions. It was found that WMA binders prepared with organic additives (Sasobit and Sasobit Redux) showed higher values of BS than their respective base asphalt binders in dry as well as wet conditions. This is attributed to the presence of crystallized wax which increases the stiffness of the binder at the ambient temperature range [366]. The effect of Rediset and Cecabase was not found to be significant in terms of BS values. In both dry and wet condition, the BS value of binders (except Sasobit) with dolomite was found to be higher than granite. This indicates that calcareous aggregates offer better binding with asphalt binder in comparison to siliceous aggregates. The extent of change in BS of different asphalt binders is also dependent on the aggregate source. For example, in the dry state, the percentage increase (with respect to the base binder, VG 30) in BS of WMA binders prepared with Sasobit and Sasobit Redux was found to be 29% and 13% respectively, while the corresponding increase was 12% and 8% with dolomite. On the other hand, in PMB 40, the percentage increase with Sasobit Redux is higher than Sasobit. Attributed to the higher stiffness, the dry BS of polymer modified blends were higher than VG30 blends. However, in the wet state their BS was found to be comparable. This also indicates that the moisture resistance inherently affected by the type of base binder.

Moisture sensitivity of asphalt binders was quantified in terms of BSR, which is the ratio of BS value in wet and dry conditions. Figure 5.27 shows the effect of WMA additives on the BSR of different asphalt binder and aggregate combinations. In general, the BSR of all the WMA blends were higher than the values of the base asphalt binders. This observation led to an important conclusion that the reduction in production temperatures of WMA do not deteriorate their moisture resistance. The

extent of improvement in BSR was higher for chemical WMAs in comparison to organic WMAs. Among all the WMA additives, Rediset showed superior moisture resistance, resulting in approximately 7-12% higher BSR, followed by Cecabase (3-8%), Sasobit Redux (3-7%), and Sasobit (0-2%).

Images of failure surface obtained in PAT can help in identifying the mode of failure (cohesive, adhesive or hybrid). AASHTO TP91 [568] has outlined the criteria for interpreting the results, as described in Table 5.4. Such identification is important to understand the compatibility between mineral aggregates and asphalt binder. Table 5.5 and Table 5.6 present the failure pattern of different asphalt binder and aggregate combinations under dry and wet conditioned states. Under the dry-conditioned state, more than 50% of the asphalt binder was coated over the aggregates for all the combinations, thus indicating cohesive failure. The primary reason for cohesive failure is the deterioration of material integrity rather than the bond between the aggregate and asphalt binder. It is usually anticipated that after moisture conditioning, the bond between aggregate and binder weakens, which may lead to adhesive failure. Interestingly, in this study it was found that none of WMA binders failed in adhesion after moisture conditioning. This indicates that WMA additives promotes improvement in bonding between aggregate and asphalt binder. Organic WMAs were found to fail in either cohesive or hybrid mode, while, chemical WMAs, irrespective of any combination, failed in cohesion. This confirms the antistripping characteristics of chemical-based WMA additives. Aggregate source was also found to affect the failure pattern. In dolomite aggregates, irrespective of the base asphalt binder, WMA technology, and conditioning process, cohesive failure was observed.

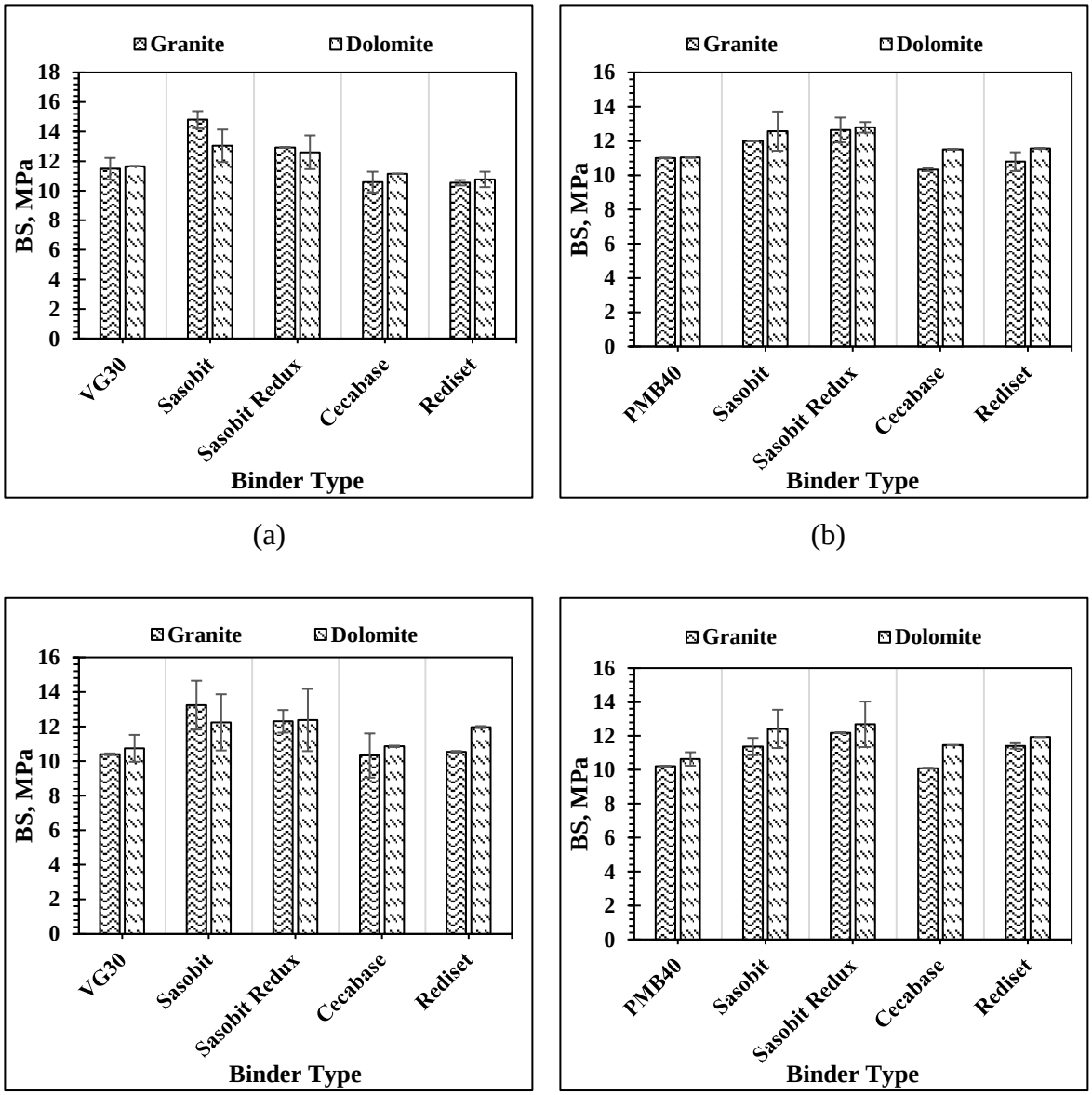


Figure 5.26. Bond strength values of WMA (a) Dry conditioned samples with VG30 as base binder, (b) Dry conditioned samples with PMB40 as base binder, (c) Wet conditioned samples with VG30 as base binder, and (d) Wet conditioned samples with PMB40 as base binder

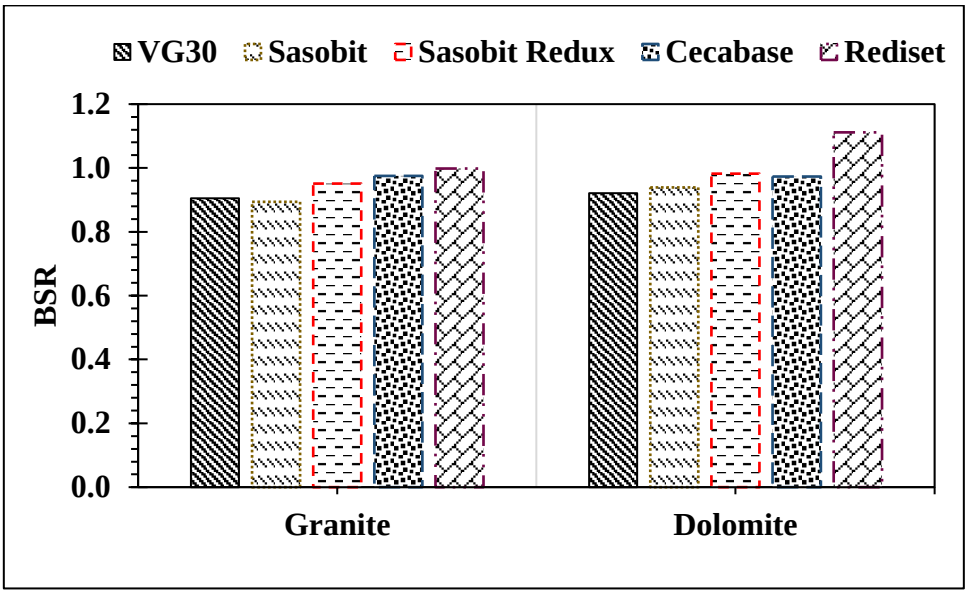


(a)

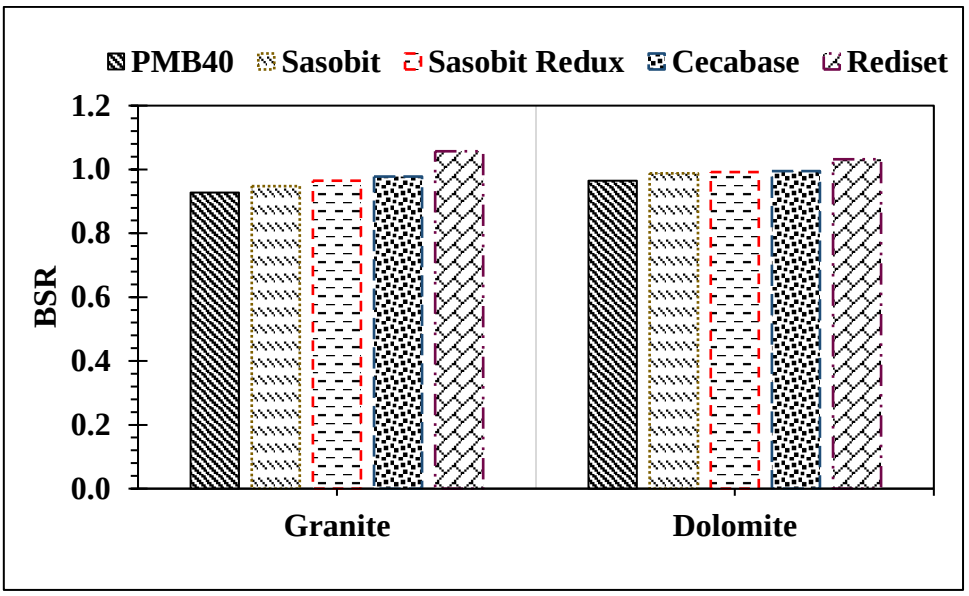


(b)

Figure 5.27. Variation in BSR with the addition of WMA additives in different base asphalt binders (a) VG30 and (b) PMB40

Table 5.4. Failure patterns and interpretation criteria

| Failure | Interpretation Criteria | Remarks | Example |
|---|---|---|---|
| **Cohesive (C)** | More than 50% of the aggregate surface remains coated with the asphalt binder. | Applied stress exceeds the cohesive strength of the asphalt binder. | 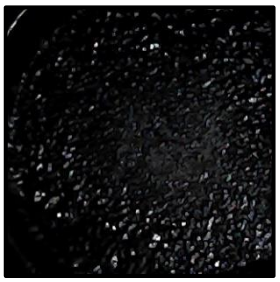 |
| **Adhesive (A)** | More than 50% of the aggregate surface is exposed. | Applied stress is higher than the interfacial BS between asphalt binder and aggregate matrix, | 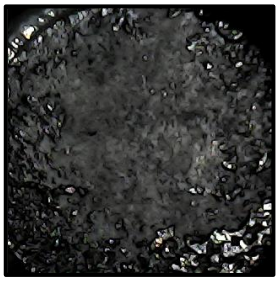 |
| **Hybrid (A/C)** | Half of the aggregate surface is covered with asphalt binder, and half of the aggregate surface is exposed. | Neither purely cohesive nor purely adhesive. | 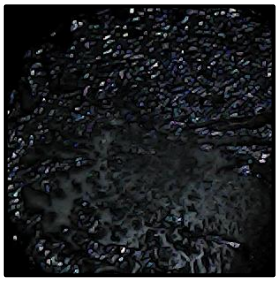 |

Table 5.5. Failure patterns when base asphalt binder is VG30

| Binder Type | Granite | | Dolomite | |
|---|---|---|---|---|
| | Dry | Wet | Dry | Wet |
| **VG30** | 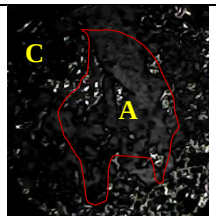 | 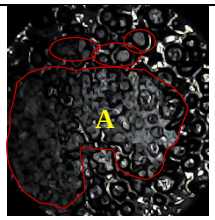 | 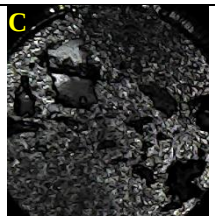 | 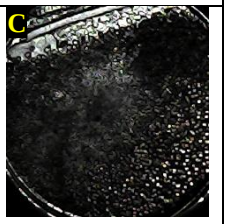 |

| | | | | |
|---|---|---|---|---|
| **S** | 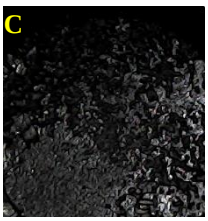 | 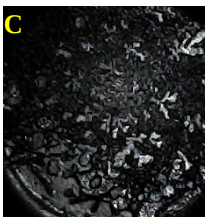 | 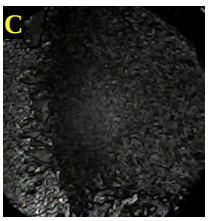 | 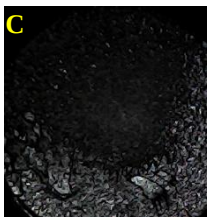 |
| **SR** | 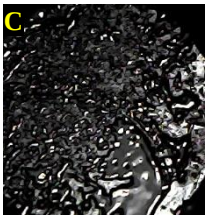 | 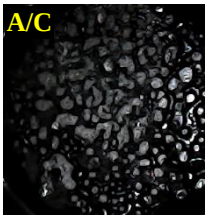 | 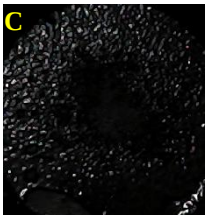 | 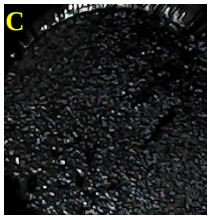 |
| **C** | 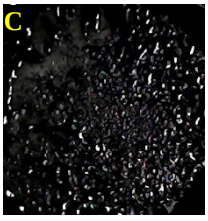 | 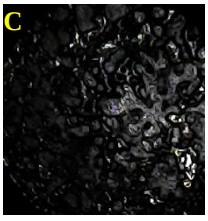 | 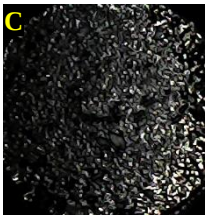 | 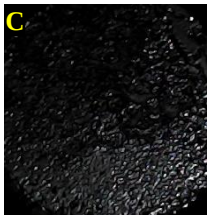 |
| **R** | 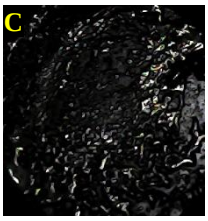 | 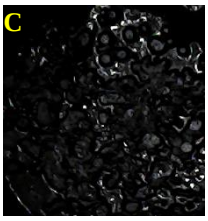 | 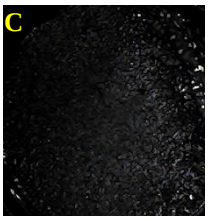 | 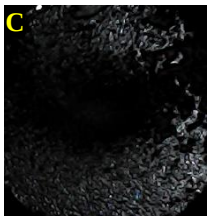 |

Table 5.6. Failure patterns when base asphalt binder is PMB40

| **Binder Type** | **Granite** | | **Dolomite** | |
|---|---|---|---|---|
| | **Dry** | **Wet** | **Dry** | **Wet** |
| **PMB40** | 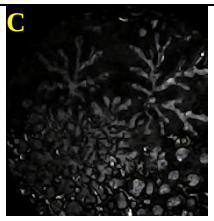 | 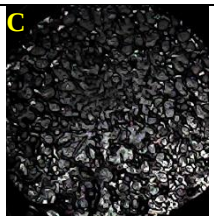 | 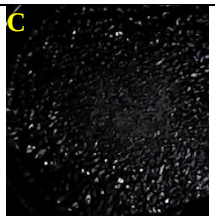 | 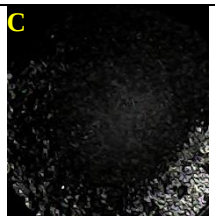 |
| **PS** | 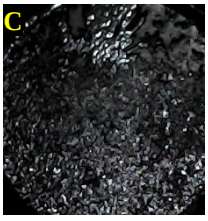 | 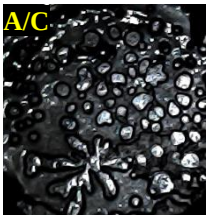 | 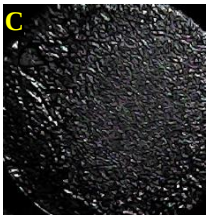 | 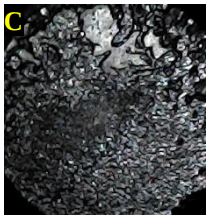 |
| **PSR** | 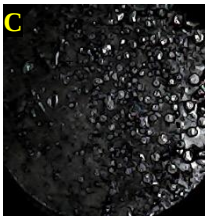 | 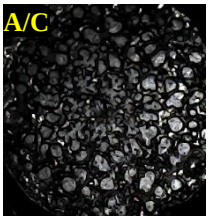 | 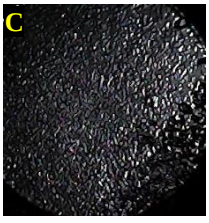 | 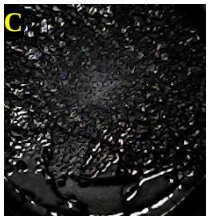 |

| | | | | |
|---|---|---|---|---|
| **PC** | 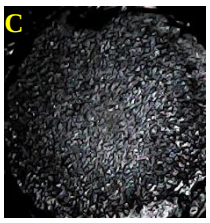 | 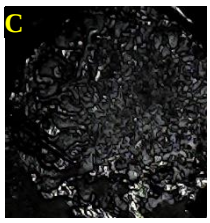 | 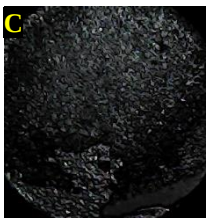 | 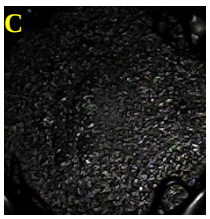 |
| **PR** | 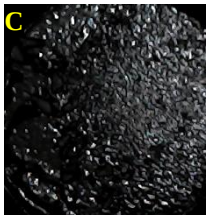 | 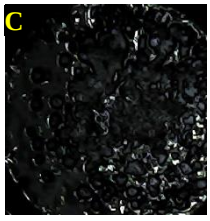 | 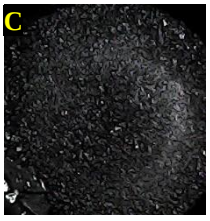 | 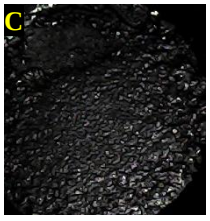 |

## 5.7 Summary

This chapter detailed the performance of WMA binders in terms of ageing, rutting, fatigue, and moisture characteristics. All the WMA binders were prepared at their optimum dosage, which was selected based on the impact of production temperatures (as described in chapter 4). Testing was done on STA and LTA samples to understand the ageing behavior of WMA binders. FTIR technique was used and different ageing indices were determined. A series of rheological tests were performed to understand the rutting and fatigue behavior. These include frequency sweep (FS) (10-70°C), multiple stress creep and recover (MSCR) (40-70°C), and Linear amplitude sweep test (LAST) (10-30°C). Further the effect of moisture damage was evaluated based on BS mechanism. The following are the salient inferences based on the experimental work and analysis conducted in this chapter:

- Ageing susceptibility of different asphalt binders was evaluated and compared based on $I_{C=O}$ and $I_{S=O}$. Among the ageing indices, $I_{S=O}$ yielded relatively higher values than $I_{C=O}$. A definite increase in the ageing indices were observed with the transition of ageing stage from STA to LTA. However, $I_{S=O}$ failed to capture the ageing effect for some of the WMA binders. All the WMA binders (STA and LTA)

displayed lower value of carbonyl index ($I_{C=O}$), indicating lower ageing susceptibility. Using WMA additives with VG30 lowered the ageing susceptibility by around 24-65%, whereas 23-57% reduction was observed in the case of PMB40.

- Superpave rutting and fatigue parameters were used to compare different asphalt binders. Master curves of $|G^*|/\sin\delta$ and $|G^*|\sin\delta$ were constructed at 60°C and 20°C, respectively. It was evident that WMA additives (except Sasobit) did not influence the rutting potential of base asphalt binders. Sasobit modified asphalt binders indicated higher value of $|G^*|/\sin\delta$, leading to improved rutting susceptibility, especially at lower frequency range. On the other hand, WMA binders with VG30, particularly organic-based, lead to higher fatigue susceptibility. Considering rutting and fatigue, the effect of WMA additives was not found to be very significant in PMB40.
- MSCR test was performed at different stress and temperature conditions to assess the rutting behaviour of WMA binders. The addition of WMA additives showed either similar or improved elastic response. Sasobit indicated higher improvement with VG30, whereas Cecabase imparted superior elasticity with PMB40. Similar to elastic response, WMA additives considerably influences the rutting behavior of base asphalt binders. Among different WMA additives, Sasobit showed excellent rutting performance (lower $J_{nr}$). At high temperatures and stress levels, all the WMA binders perform similar or even better than base asphalt binders.
- Another parameter, which combines the effect of temperature and stress levels, was chosen to rank the rutting resistance of asphalt binders. The parameter, typically defined as rutting parameter (RP), was determined based on the concept of Arrhenius energy. Based on RP, the addition of WMA additives in VG30 (except

Sasobit) exhibit comparable high temperature performance. However, the impact of WMA was lower in case of PMB40.

- Stress-strain plots were used to identify the strain dependency of WMA binders at different temperatures (10, 20, and 30°C). Despite higher peak stresses, the inclusion of WMA additives in VG30 improved the strain tolerance. With the dominance of polymeric network in PMB40, the effect of WMA additives was not evident. On an average, organic additives improved the peak stress, whereas chemical agents lead to higher failure strain.
- Fatigue resistance of asphalt binders was determined and compared using LAST at 10, 20, and 30°C. No definite trend was identified in LAST fatigue parameters (*A* and *B)* with the change in WMA additive. Chemical-based WMA binders displayed superior fatigue performance throughout the strain amplitudes. Fatigue curves clearly showed the high strain susceptibility of Sasobit modified asphalt binders. Nonetheless, it was evident that WMA binders does not deteriorate the fatigue behavior of asphalt binders, irrespective of test temperature and base asphalt binder.
- The moisture susceptibility of asphalt binders was evaluated using Pneumatic adhesion test (PAT). The moisture resistance (in terms of BSR) of asphalt binders improved with the incorporation of WMA additives. Rediset outperformed among other WMA additives, resulting in approximately 7-12% higher BSR, followed by Cecabase (3-8%), Sasobit Redux (3-7%), and Sasobit (0-2%). Besides, none of the WMA binders failed in adhesion after moisture conditioning.